

NOTICE

This report was prepared as an account of work sponsored by an agency of the United States Government. Neither the United States Government nor any agency thereof, or any of their employees, makes any warranty, expressed or implied, or assumes any legal liability or responsibility for any third party's use, or the results of such use, of any information, apparatus, product or process disclosed in this report, or represents that its use by such third party would not infringe privately owned rights.

The views expressed in this report are not necessarily those of the U.S. Nuclear Regulatory Commission.

LOW-LEVEL WASTE PACKAGE AND ENGINEERED-BARRIER STUDY

QUARTERLY PROGRESS REPORT

JANUARY - MARCH 1988

P. Soo
B. S. Bowerman
J. H. Clinton
L. Milian

Nuclear Waste and Materials Technology Division
Department of Nuclear Energy
Brookhaven National Laboratory
Upton, New York 11973

June 1988

NOTICE: This document contains preliminary information and was prepared primarily for interim use. Since it may be subject to revision or correction and does not represent a final report, it should not be cited as reference without the expressed consent of the author(s).

Prepared for the U.S. Nuclear Regulatory Commission
Office of Nuclear Regulatory Research
Contract No. DE-AC02-76CH00016
FIN A-3291

ABSTRACT

Gamma-irradiation and sulfate-attack tests were continued on Portland I, Portland V, and Ontario-Hydro-type cement mortars to determine their suitability as low-level waste barriers. Gamma doses to 1.0×10^9 rad do not seem to detrimentally affect compressive strength. For the sulfate-attack studies, the Ontario-Hydro-type composition, which included silica fume, showed the least resistance to attack, followed by Portland I type cement-mortar.

Mechanical property tests are being carried out on high-density polyethylene to determine which failure/degradation modes could be important if this material is used for waste containers. Irradiation-embrittlement tests are also being performed on stressed U-bend specimens to estimate the rates of crack initiation and propagation.

CONTENTS

	<u>Page</u>
ABSTRACT	111
LIST OF FIGURES	vii
LIST OF TABLES	ix
ACKNOWLEDGMENTS	xi
1. INTRODUCTION	1
2. MECHANICAL AND CHEMICAL STABILITY OF CEMENT-BASED STRUCTURAL MATERIALS	3
2.1 Sulfate-Attack Tests	3
2.2 Gamma-Irradiation Tests	12
3. DEGRADATION MECHANISMS IN HIGH-DENSITY POLYETHYLENE (HDPE)	19
3.1 Overview of Research Activities	19
3.2 Crack Initiation and Propagation in a Gamma-Radiation Environment	19
3.3 Crack Initiation and Propagation in Chemical Environments . .	21
3.4 Uniaxial Creep Behavior	31
3.5 Testing Protocol for HDPE	31
3.6 Publications on HDPE Research	39
4. BIODEGRADATION OF ION-EXCHANGE MEDIA	41
5. REFERENCES	43
6. APPENDICES	

LIST OF FIGURES

	<u>Title</u>	<u>Page</u>
Figure 2.1	Comparison of 25.4 cm (10 in) long Portland I cement mortar-bars after 115 wet/dry cycles in 2.1% Na ₂ SO ₄ solution and deionized water.	6
Figure 2.2	Side views of the Portland I cement-mortar samples shown in Figure 2.1	7
Figure 2.3	Comparison of 25.4 cm (10 in) long Portland V cement-mortar bars after 105 wet/dry cycles in 2.1% Na ₂ SO ₄ solution and deionized water.	8
Figure 2.4	Side views of the Portland V cement-mortar samples shown in Figure 2.3	9
Figure 2.5	Comparison of 25.4 cm (10 in) long OHCM cement-mortar bars after 159 wet/dry cycles in 2.1% Na ₂ SO ₄ solution and deionized water	10
Figure 2.6	Side views of the OHCM cement-mortar samples shown in Figure 2.5	11
Figure 2.7	Compressive Strength of Portland I cement-mortar as a function of cure time and gamma irradiation.	15
Figure 2.8	Compressive Strength of Portland V cement-mortar as a function of cure time and gamma irradiation.	16
Figure 2.9	Compressive Strength of OHCM as a function of cure time and gamma irradiation	17
Figure 3.1	Crack patterns formed in the apex regions of Marlex CL-100 HDPE U-bend specimens prior to long-term exposure to air	22
Figure 3.2	Crack patterns in the HDPE U-bend specimens shown in Figure 3.1 after 227 d exposure to air at 20°C	23
Figure 3.3	Crack patterns formed in the apex regions of Marlex CL-100 HDPE U-bend specimens prior to long-term exposure to deionized water	24
Figure 3.4	Crack patterns in the HDPE U-bend specimens shown in Figure 3.3 after 227 d exposure to deionized water at 20°C	25

LIST OF FIGURES (continued)

	<u>Title</u>	<u>Page</u>
Figure 3.5	Crack patterns formed in the apex regions of Marlex CL-100 HDPE U-bend specimens prior to long-term exposure to nitrogen.	26
Figure 3.6	Crack patterns in the U-bend specimens shown in Figure 3.5 after 227 d exposure to nitrogen at 20°C	27
Figure 3.7	Crack patterns formed in the apex regions of Marlex CL-100 HDPE U-bend specimen prior to long-term exposure to a vacuum.	28
Figure 3.8	Crack patterns in the U-bend specimens shown in Figure 3.7 after 227 d exposure to initial vacuum conditions	29
Figure 3.9	Elongations at failure for Marlex CL-100 HDPE tested at 20°C in various environments	38

LIST OF TABLES

	<u>Title</u>	<u>Page</u>
Table 2.1	Length increase measurements on cement-mortar bars exposed to alternate wet-dry cycling in 2.1% Na ₂ SO ₄ solution or deionized water.	4
Table 2.2	Densities of cement-mortar bars used in sulfate-attack tests	12
Table 2.3	Effect of gamma irradiation on the compressive strength of cement-mortars	14
Table 3.1	Test matrix for crack-propagation studies on irradiated Marlex CL-100 miniature U-bend specimens.	20
Table 3.2	Cracking in Type I HDPE U-bend specimens exposed for 227 d to various test environments	30
Table 3.3	Creep test data for Marlex CL-100 HDPE tested in air and deionized water at room temperature.	32
Table 3.4	Creep test data for Marlex CL-100 HDPE tested in various environments at room temperature	33
Table 3.5	Irradiation-creep test matrix for HDPE	34

ACKNOWLEDGMENTS

The authors express their appreciation to Ms. T. Skelaney and Ms. A. Lopez for the preparation of this report.

1. INTRODUCTION

Since the publication of NRC Rule 10 CFR 61, "Licensing Requirements for Land Disposal of Radioactivity Wastes," and the NRC Technical Position on Waste Form, there has been action by industry to develop improved low-level waste forms, containers, and engineered barriers. Over the last several years the NRC received a large number of Topical Reports for review as a part of license applications for waste forms, containers, and engineered barriers. During review of the reports, it was recognized that the data provided by the vendors are usually insufficient or questionable. It was also recognized that conventional test methods, such as ASTM test procedures, may not be applicable to certain waste package materials and that analytical procedures have not been established to interpret the test data with respect to the performance objectives in the regulation.

The objective of this research project is to develop an adequate data base for performance review of low-level waste package materials identified in vendors' topical reports and to provide a basis for technical guidance to States and applicants. This project will also review and improve, if needed, the existing tests methods for application to materials and to the design of waste packages and engineered barrier concepts. Methods will be developed to extrapolate short-term test data to long-term performance of waste packages as required in the regulation.

To date, five research tasks have been specified by NRC and BNL. They include:

- Task 1: Development of Work Plan.
- Task 2: Mechanical and Chemical Stability of Concrete-Based Structural Materials.
- Task 3: Degradation Mechanisms in High-Density Polyethylene (HDPE).
- Task 4: Biodegradation of Ion-Exchange Media.
- Task 5: Development of HDPE Testing Protocol.

Task 1 has been completed. Work in Task 2 is at an advanced stage, but will be significantly curtailed after this reporting period because of reduced funding. Task 3 is continuing on the long-term creep behavior of HDPE. Data from this study will be used in Task 5 which began this quarter. Experimental work in Task 4 has been completed and a Topical Report is being finalized.

2. MECHANICAL AND CHEMICAL STABILITY OF CEMENT-BASED STRUCTURAL MATERIALS

Three types of cementitious material were prepared for this study, including Portland I and V, and a formulation prepared from information received from Ontario Hydro. This is designated Ontario Hydro-type cement mortar (OHCM), although it should be stated that such laboratory-sized specimens may not accurately simulate the actual material. These materials are used for both sulfate-attack and gamma-irradiation tests. Details of specimen preparation and testing were given in a previous quarterly report (Soo, and others, 1987).

2.1 Sulfate - Attack Tests

These are accelerated tests to determine the susceptibility of cementitious barrier materials to deterioration from sulfates which are present in soils in contact with the cement. The BNL procedure is based on that developed by Kalousek (1976). He showed that sulfate attack effects could be accelerated by a factor of eight if alternate wet-dry cycling of samples was adopted in place of continuous immersion in sulfate solution. The drying cycle evaporates water in the cement matrix and allows fresh sulfate solution to enter during reimmersion. Without the drying period, sulfate would penetrate more slowly into the cement pores by a diffusional process. Four replicate mortar bars were used for both the sulfate-attack tests and their corresponding controls.

The BNL immersion/drying cycle is:

Step 1: Immersion of specimens in 2.1% Na_2SO_4 solution (or deionized water for the control tests) at room temperature for 16 h.

Step 2: Forced-air drying of the specimens for 7 h 40 min at $54 \pm 1^\circ\text{C}$.

Step 3: 20 min cooling of the specimens in still air.

Step 4: Repeat Step 1 through 4.

All testing begins with an immersion cycle with specimens (measuring 25.4 x 2.54 x 2.54 cm) placed in plastic containers of Na_2SO_4 solution (or deionized water). Glass rods are placed on the bottoms of the containers to assure solution contact on all sides of the test bars. During weekends the samples are left in the immersion cycle and they accumulate 64 h of soaking during this period.

A second set of length-change measurements was performed during this quarter. The readings were taken from a dial gage on a special comparator which records changes in length rather than absolute lengths of the specimens. A description of the comparator may be found in ASTM Standard C490 - "Apparatus for Use in Measurement of Length Change of Hardened Cement Paste, Mortar and Concrete." Data obtained are given in Table 2.1.

Table 2.1 Length increase measurements on cement mortar bars exposed to alternate wet-dry cycling in 2.1% Na₂SO₄ solution or deionized water.

Specimen	Test Solution	Test Time(d)	Number of Cycles	Initial Dial Gage Reading (in)	Final Dial Gage Reading (in)	Length Change(in)	% Change (1)
<u>Portland I</u>							
1	DIW	71	48	0.1810	0.1810	0.0010	0.01
2	DIW	71	48	0.1785	0.1785	0.0005	0.01
4	DIW	71	48	0.1770	0.1770	0.0005	0.01
5	DIW	71	48	0.1740	0.1740	0.0005	0.01
1	DIW	180	115	0.1810	0.1810	0.0010	0.01
2	DIW	180	115	0.1785	0.1795	0.0010	0.01
4	DIW	180	115	0.1770	0.1780	0.0010	0.01
5	DIW	180	115	0.1740	0.1745	0.0005	0.01
8	Na ₂ SO ₄	71	48	0.0470	0.0715	0.0245	0.25
9	Na ₂ SO ₄	71	48	0.0335	0.0580	0.0245	0.25
10	Na ₂ SO ₄	71	48	0.1780	0.2000	0.0220	0.22
11	Na ₂ SO ₄	71	48	0.1800	0.2010	0.0210	0.21
8	Na ₂ SO ₄	180	115	0.0470	0.2480	0.2010	2.01
9	Na ₂ SO ₄	180	115	0.0335	0.2320	0.1985	1.99
10	Na ₂ SO ₄	180	115	0.1780	0.3730	0.1950	1.95
11	Na ₂ SO ₄	180	115	0.1800	0.3710	0.1910	1.91
<u>Portland V</u>							
1	DIW	69	45	0.1605	0.1595	-0.0010	-0.01
2	DIW	69	45	0.1625	0.1615	-0.0010	-0.01
3	DIW	69	45	0.0470	0.0460	-0.0010	-0.01
4	DIW	69	45	0.0340	0.0330	-0.0010	0.01
1	DIW	166	105	0.1605	0.1610	0.0005	0.01
2	DIW	166	105	0.1625	0.1630	0.0005	0.01
3	DIW	166	105	0.0470	0.0475	0.0005	0.01
4	DIW	166	105	0.0340	0.0340	0	0
5	Na ₂ SO ₄	69	45	0.1845	0.1895	0.0050	0.05
6	Na ₂ SO ₄	69	45	0.1790	0.1835	0.0045	0.05
7	Na ₂ SO ₄	69	45	0.0270	0.0335	0.0065	0.07
8	Na ₂ SO ₄	69	45	0.0550	0.0605	0.0055	0.06
5	Na ₂ SO ₄	166	105	0.1845	0.2180	0.0335	0.34
6	Na ₂ SO ₄	166	105	0.1790	0.2125	0.0335	0.34
7	Na ₂ SO ₄	166	105	0.0270	0.0745	0.0475	0.48
8	Na ₂ SO ₄	166	105	0.0550	0.0990	0.0440	0.44
<u>Ontario Hydro Type</u>							
2	DIW	74	44	0.1710	0.1770	0.0060	0.06
4	DIW	74	44	0.0445	0.0515	0.0070	0.07
5	DIW	74	44	0.1600	0.1665	0.0065	0.07
6	DIW	74	44	0.1525	0.1580	0.0055	0.06
2	DIW	159	100	0.1710	0.1815	0.0105	0.11
4	DIW	159	100	0.0445	0.0565	0.0120	0.12
5	DIW	159	100	0.1600	0.1720	0.0120	0.12
6	DIW	159	100	0.1525	0.1630	0.0105	0.11
7	Na ₂ SO ₄	74	44	0.0250	0.0690	0.0430	0.43
8	Na ₂ SO ₄	74	44	0.0410	0.0875	0.0465	0.47
9	Na ₂ SO ₄	74	44	0.1565	0.1900	0.0335	0.34
11	Na ₂ SO ₄	74	44	0.0300	0.0800	0.0500	0.50
7	Na ₂ SO ₄	159	100	0.0250	0.3030	0.0278	2.78
8	Na ₂ SO ₄	-	-	0.0410	-(2)	-	-
9	Na ₂ SO ₄	159	100	0.1565	0.3915	0.235	2.35
11	Na ₂ SO ₄	-	-	0.0300	-(2)	-	-
<u>Note:</u>							
(1) Based on an effective gage length of 10.00 in.							
(2) No measurement performed because mortar bar fractured during immersion/oven transfer.							

Portland I cement mortar shows little expansion in deionized water (DIW) after accumulating 115 cycles in a period of 180 d. When this material is exposed to a 2.1 weight percent Na_2SO_4 solution, however, the specimens show large amounts of expansion from the sulfate-attack process. The rate of expansion is initially small (about 0.23 percent after 48 cycles) but it rapidly increases to approximately 2.0 percent (after 115 cycles) as specimen cracking occurs, allowing faster ingress of sulfate into the cement.

Portland V cement is designed to be more resistant to sulfate attack. Little change in length is noticed for DIW immersion, as would be expected. In the sulfate-solution tests there is significant expansion but it is only about 20 percent of that for Portland I material.

The OHCM bars continued to show surprisingly poor sulfate-attack resistance. After 159 cycles the expansion is about 2.5 percent. Two test bars were so badly cracked that they fractured into two pieces during transfer to the drying oven. Even deionized water caused the OHCM specimens to swell at a rate much higher than those for Portlands I and V mortar bars. That OHCM can swell from exposure to pure water indicates that swelling may not be totally attributable to sulfate attack.

Figures 2.1 through 2.6 show photographs of the different types of mortar bar after accumulating the 100-115 test cycles described in Table 2.1. For Portland I samples the length increase for the sulfate-immersed sample is clearly seen in comparison to the DIW control bar (Figures 2.1 and 2.2). Little porosity is seen from the "top surfaces" of the bars (Figure 2.1) which were the uppermost surfaces during casting of the specimens into their molds. More porosity is observed from a "side view" shown in Figure 2.2. Note the fine cracking in areas close to the edges of the specimens.

Portland V specimens show behavior similar to that for Portland I, but the expansion caused by sulfate attack is far less obvious (Figures 2.3 and 2.4). Edge cracking is also less than that for Portland I.

The photographs for the OHCM (Figures 2.5 and 2.6) show the large amount of expansion from sulfate attack. Edge cracking is seen together with major cracking normal to the major axis of the bar. Compared to the Portland I and V specimens there is a larger amount of porosity, which may contribute to the ingress of sulfate solution and expansion. Nevertheless, the large amount of expansion and cracking is still surprising because the cement used in the OHCM specimens is sulfate-resistant Portland V. Quite possibly a reduction in the amount of porosity will reduce the amount of sulfate attack. However, in the preparation of the current test specimens care was taken not to tamp the cast mortar too vigorously to remove air bubbles since there is the danger of causing the sand component to settle to the bottom of the mold. This would give a non-homogeneous mix.

Although the test bars show differences in porosity, actual density measurements on the as-cast bars do not reflect this. Table 2.2 shows density values for specimens made from the three different formulations. The density of each is in the 2.15 to 2.16 g/cc range.

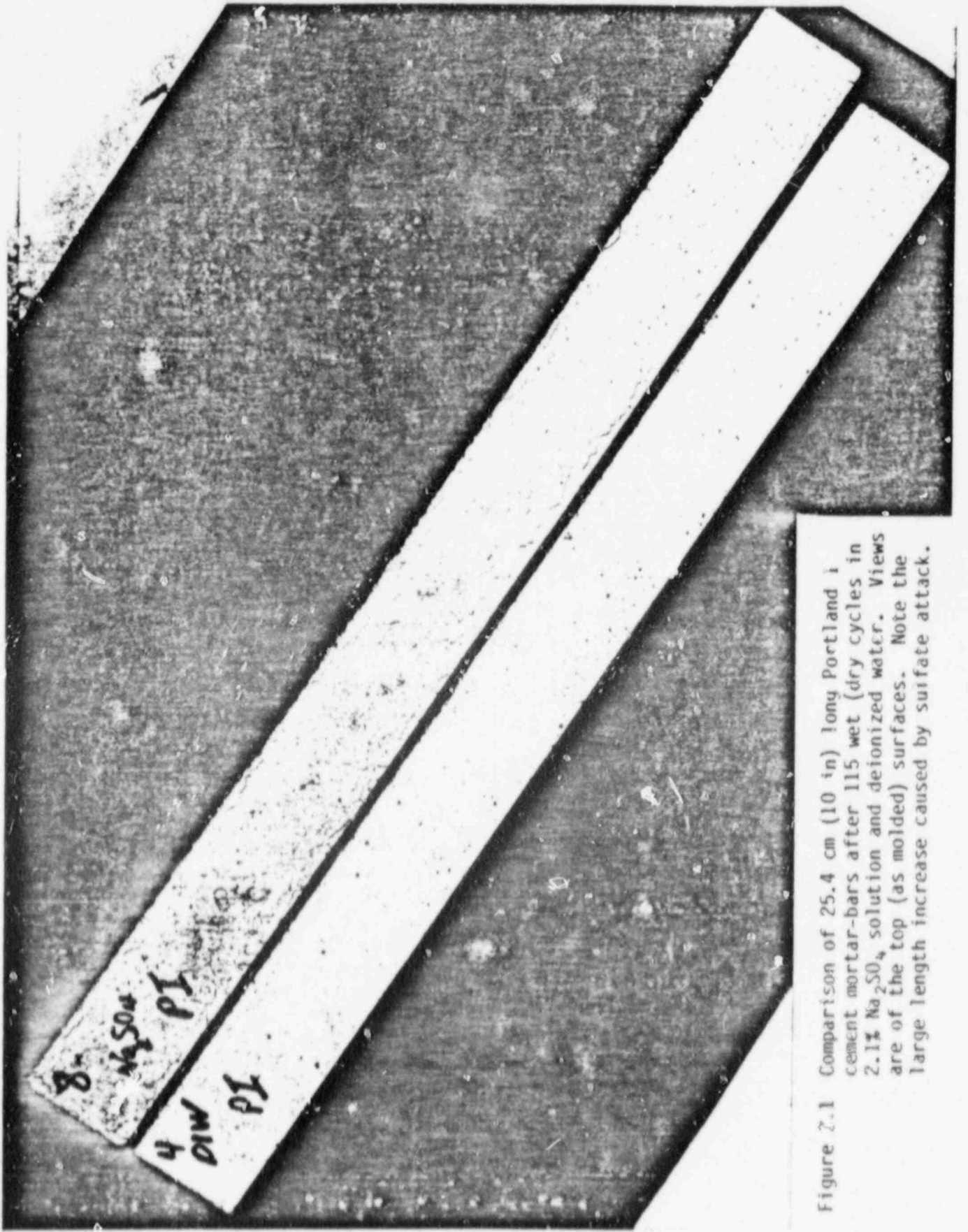


Figure 7.1 Comparison of 25.4 cm (10 in) long Portland i cement mortar-bars after 115 wet (dry cycles in 2.1% Na_2SO_4 solution and deionized water. Views are of the top (as molded) surfaces. Note the large length increase caused by sulfate attack.

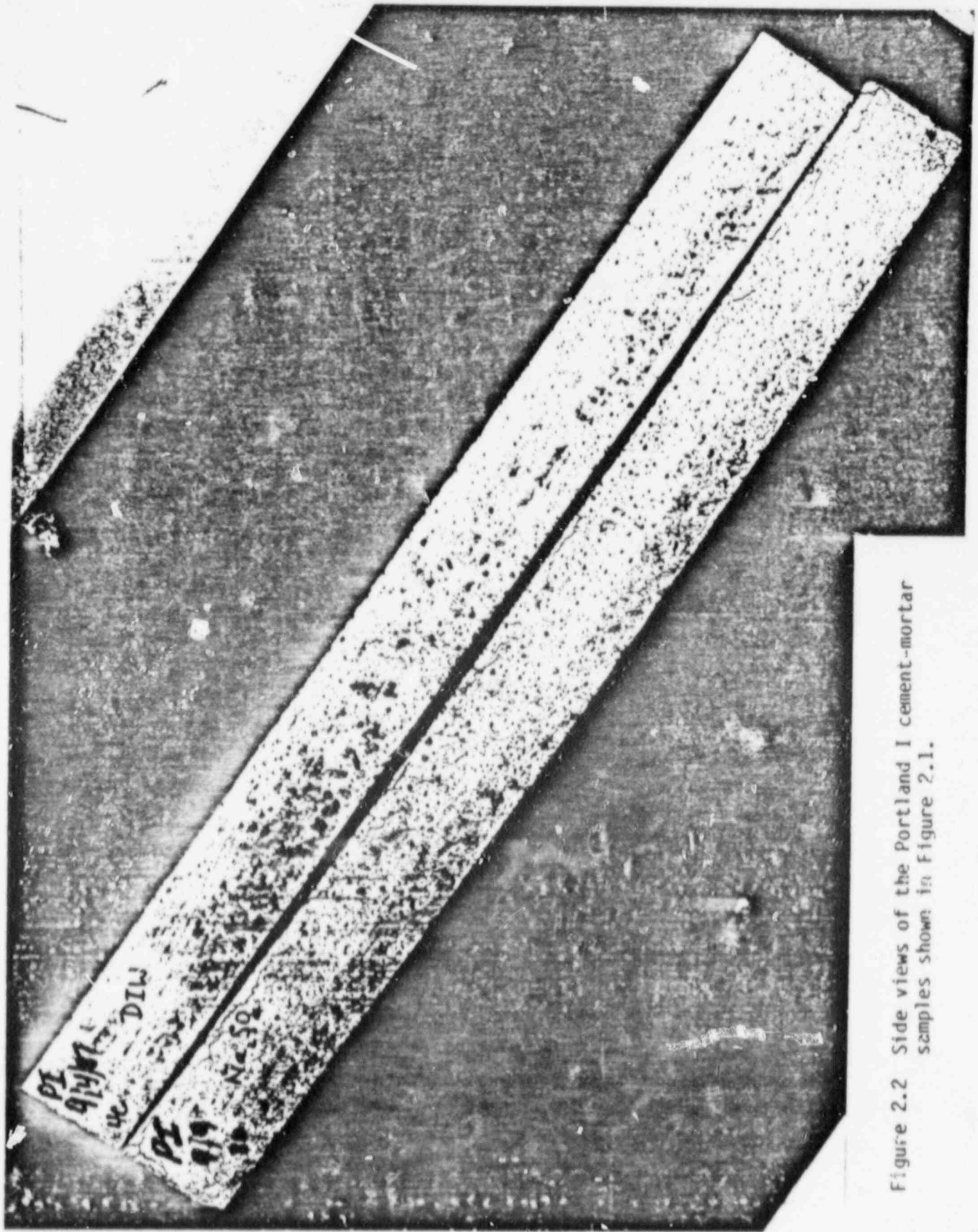


Figure 2.2 Side views of the Portland I cement-mortar samples shown in Figure 2.1.

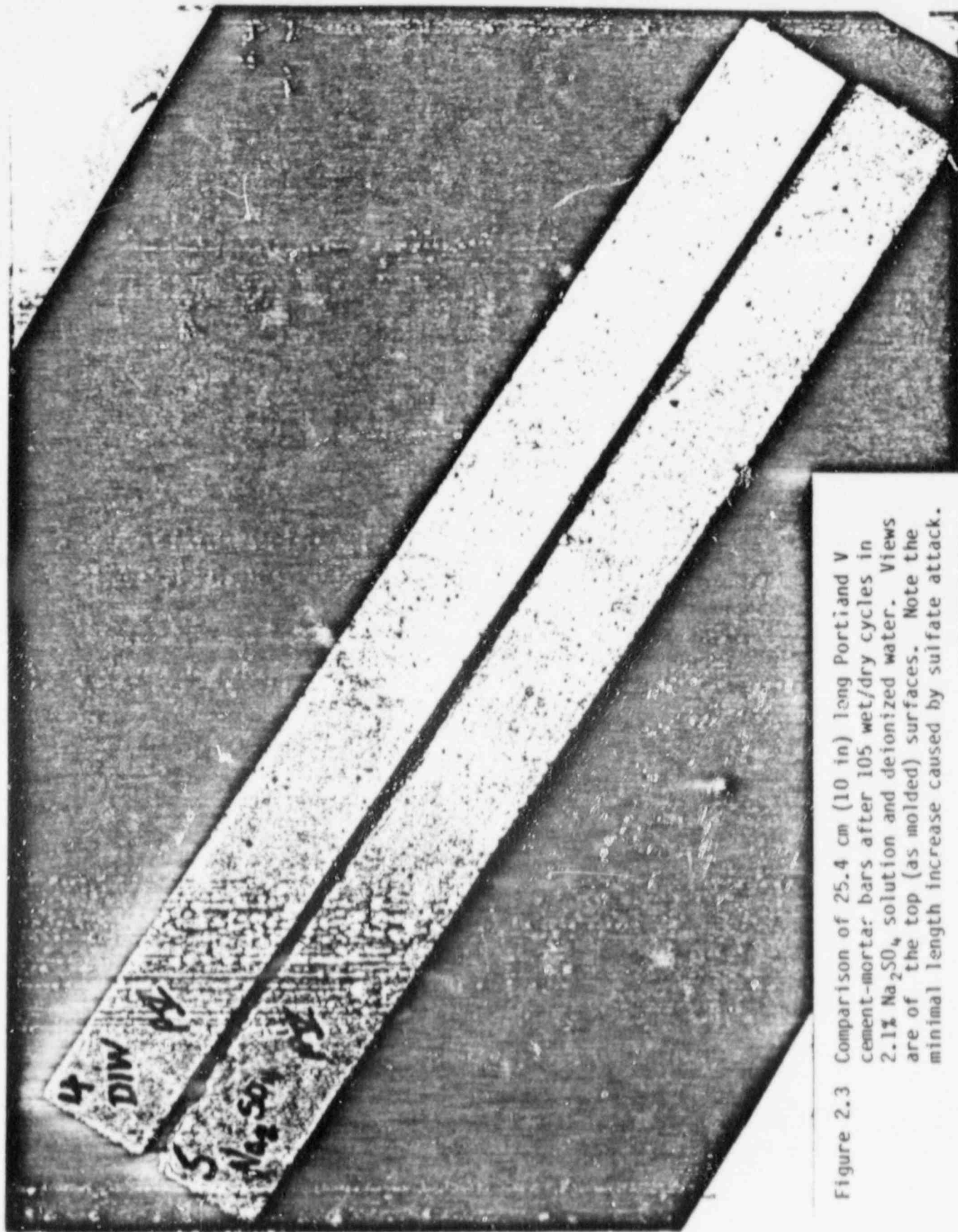


Figure 2.3 Comparison of 25.4 cm (10 in) long Portland V cement-mortar bars after 105 wet/dry cycles in 2.1% Na_2SO_4 solution and deionized water. Views are of the top (as molded) surfaces. Note the minimal length increase caused by sulfate attack.

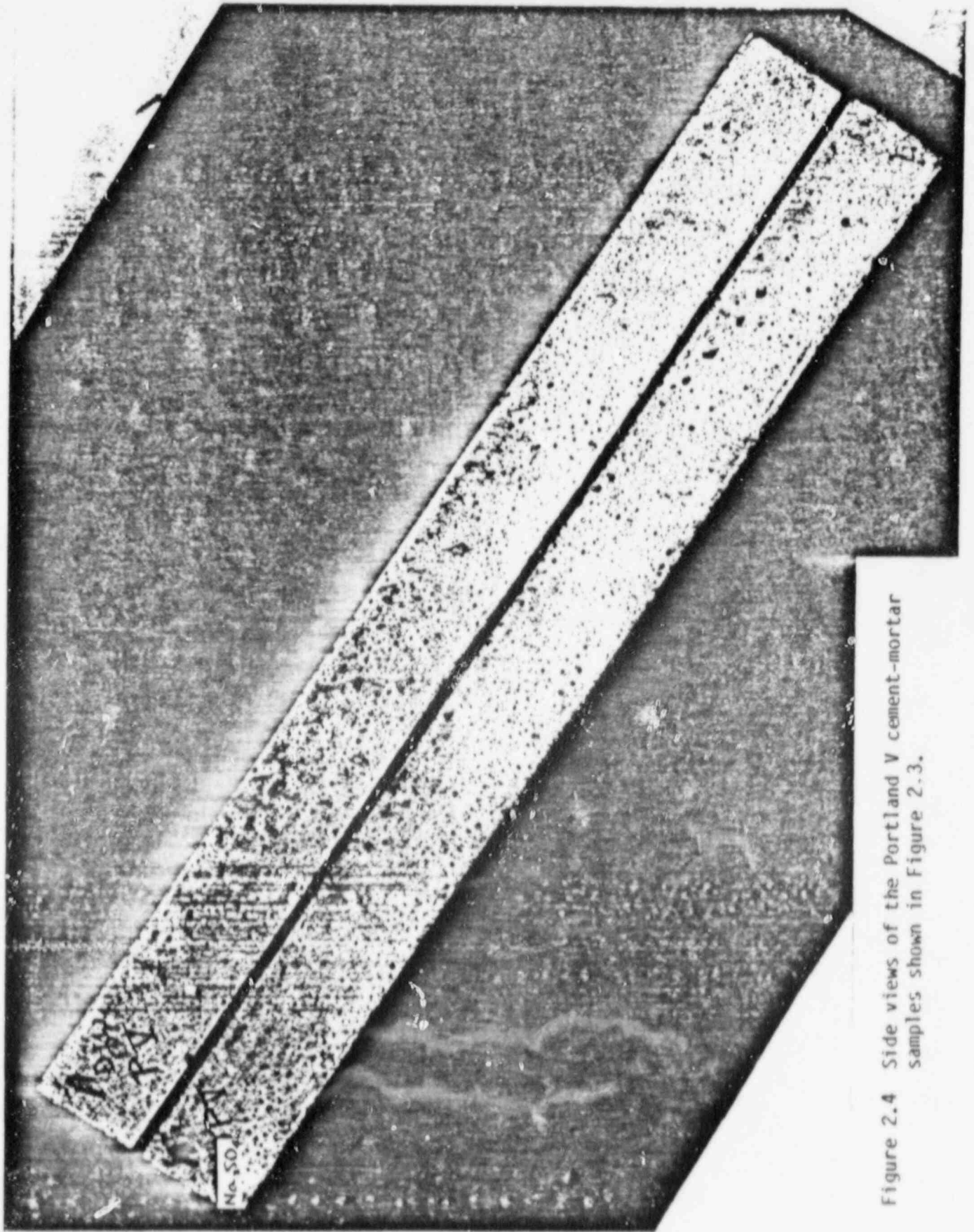


Figure 2.4 Side views of the Portland V cement-mortar samples shown in Figure 2.3.

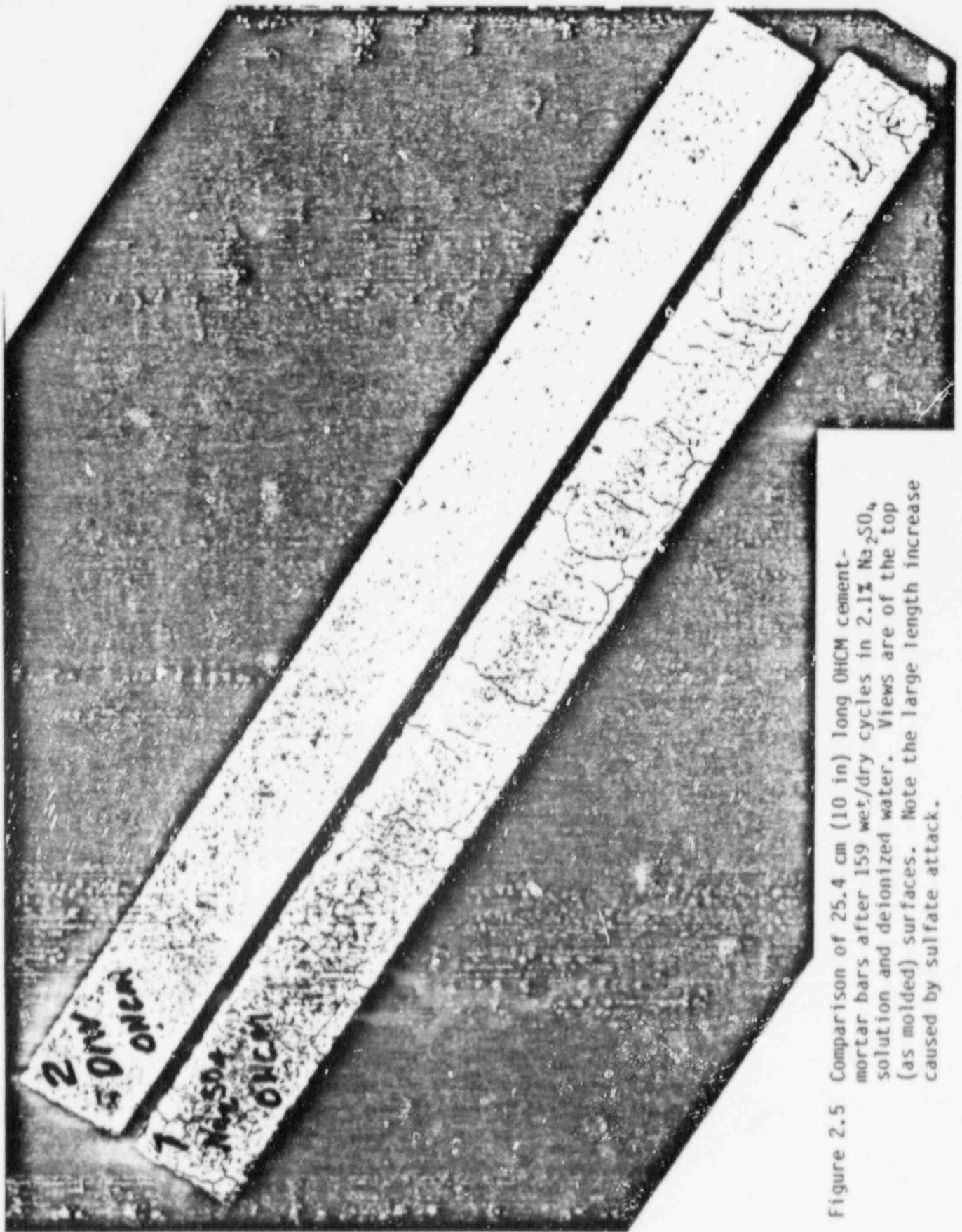


Figure 2.5 Comparison of 25.4 cm (10 in) long OHCM cement mortar bars after 159 wet/dry cycles in 2.1% Na_2SO_4 solution and deionized water. Views are of the top (as molded) surfaces. Note the large length increase caused by sulfate attack.

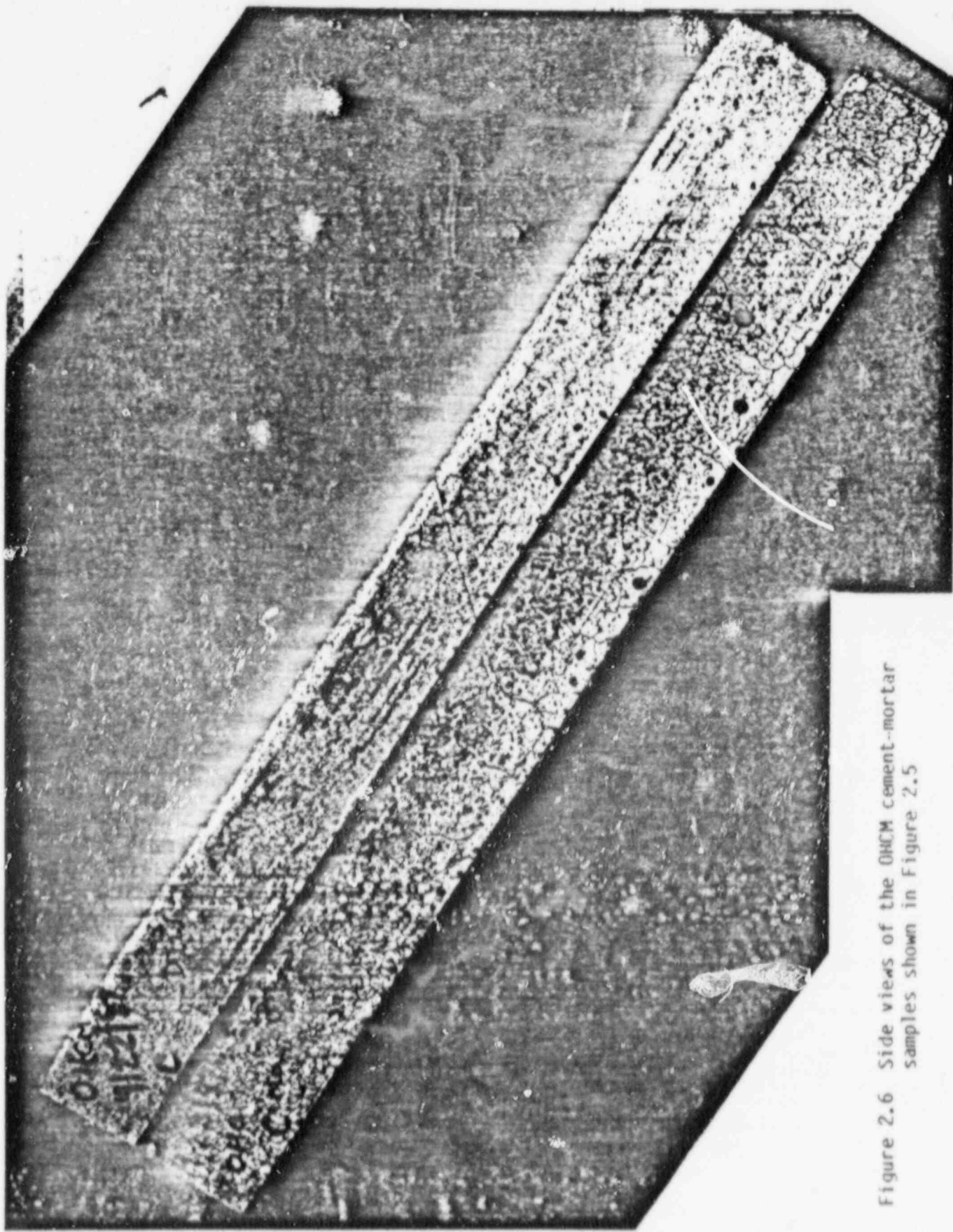


Figure 2.6 Side views of the OHCM cement-mortar samples shown in Figure 2.5

Table 2.2 Densities of cement-mortar bars used in sulfate-attack tests.

Cement-Mortar Type	Density (g/cc)
Portland I	2.15
	2.16
	2.13
	2.15
	2.17
	2.16
	Ave. <u>2.15</u>
Portland V	2.15
	2.16
	2.16
	2.16
	2.16
	Ave. <u>2.16</u>
OHCM	2.17
	2.14
	2.14
	2.13
	2.17
	Ave. <u>2.15</u>

This sulfate-attack effort is now being terminated and final results will shortly be published.

2.2 Gamma-Irradiation Tests

The test materials were identical to the formulations used in the sulfate-attack tests. The specimens were (2.54 cm) 1 in. cubes prepared similarly to the 25.4 cm (10 in.) bars. A sufficient number of samples was prepared so that compression tests could be conducted on unirradiated control samples maintained at approximately 10°C (the gamma-irradiation temperature), at room temperature, as well as on the irradiated specimens. Full details of the sample preparation and irradiation are given elsewhere (Soo, and others, 1987). Because of the limited space available in the gamma irradiation tubes, the samples had to be small (2.54 cm cubes) and only two replicates were tested for each irradiation condition. In the cases of the non-irradiated controls between 3 to 5 samples were evaluated.

Table 2.3 gives the compression test data obtained through this reporting period. Generally, the Portland V specimens are stronger than Portland I, and the OHCM specimens are far stronger than both the Portland cement mortars. Figures 2.7 through 2.9 show compressive strengths for the three materials as a function of curing time at 10° and 20°C. Since the irradiated specimens were exposed to air at about 10°C, it is assumed that they are being cured at the same time they are being irradiated. Therefore, the compression strengths for the irradiated specimens are also plotted versus the irradiation (i.e., curing) time. Typical Portland cement behavior is noticed in that close-to-full strength is achieved after 28 d of curing. The specimens irradiated for the longest time (182 d) at 3.1×10^3 rad/h always have a lower strength than the unirradiated controls. However, the differences usually fall within the uncertainty of the measurements and may not be statistically significant. At the higher dose rate there is no loss in strength compared to the unirradiated samples, even though doses up to 10^9 rad have been achieved.

The irradiations are continuing, but the work will be terminated within the next reporting period.

Table 2.3 Effect of gamma irradiation on the compressive strength of cement mortars.

Cement Type	Gamma Dose (rad)	Dose Rate (rad/h)	Cure (Irrad.) Time (d)(1)	Cure (Irrad.) Temp. (°C)	Strength ⁽²⁾	
					(psi)	(MPa)
Portland I	0	0	7	20	4170 ± 552	28.8 ± 3.1
	0	0	28	20	5675 ± 487	39.1 ± 3.4
	0	0	48.5	20	5310 ± 164	36.6 ± 1.1
	0	0	110.5	20	6810 ± 164	47.0 ± 1.1
	0	0	182	20	6590 ± 738	45.4 ± 5.1
	0	0	48.5	10	5045 ± 733	34.8 ± 5.1
	0	0	110.5	10	6383 ± 401	44.0 ± 2.8
	0	0	182	10	5933 ± 176	40.9 ± 1.2
	1.4 × 10 ⁷	3.1 × 10 ³	182	10	5125 ± 35	35.3 ± 0.2
	4.4 × 10 ⁸	4.3 × 10 ⁵	48.5	10	5150 ± 71	35.5 ± 0.5
	1.0 × 10 ⁹	4.3 × 10 ⁵	110.5	10	6325 ± 177	43.6 ± 1.2
	Portland V	0	0	7	20	3570 ± 148
0		0	28	20	5850 ± 302	40.3 ± 2.1
0		0	48.5	20	5380 ± 252	37.1 ± 1.7
0		0	110.5	20	6930 ± 115	47.8 ± 0.8
0		0	182	20	6455 ± 498	44.5 ± 3.4
0		0	48.5	10	5483 ± 76	37.8 ± 0.5
0		0	110.5	10	6917 ± 544	47.7 ± 3.8
0		0	182	10	6925 ± 11	47.8 ± 2.9
1.4 × 10 ⁷		3.1 × 10 ³	182	10	6150 ± 99	42.4 ± 6.8
4.4 × 10 ⁸		4.3 × 10 ⁵	48.5	10	5925 ± 248	40.9 ± 1.7
1.0 × 10 ⁹		4.3 × 10 ⁵	110.5	10	7100 ± 141	49.0 ± 1.0
OH ₁		0	0	7	20	5670 ± 601
	0	0	28	20	8650 ± 280	59.6 ± 1.9
	0	0	48.5	20	8320 ± 641	57.4 ± 4.4
	0	0	110.5	20	8210 ± 641	56.6 ± 4.4
	0	0	182	20	9700 ± 705	66.9 ± 4.9
	0	0	48.5	10	8283 ± 757	57.1 ± 5.2
	0	0	110.5	10	7467 ± 723	51.5 ± 5.0
	0	0	182	10	8617 ± 425	59.4 ± 2.9
	1.4 × 10 ⁷	3.1 × 10 ³	182	10	8375 ± 530	57.7 ± 3.7
	4.4 × 10 ⁸	4.3 × 10 ⁵	48.5	10	8150 ± 71	56.2 ± 0.5
	1.0 × 10 ⁹	4.3 × 10 ⁵	110.5	10	8050 ± 1131	55.5 ± 7.8

Notes: 1) For unirradiated controls the cure time is the time between cement casting and testing. For irradiated specimens it is the irradiation time.

2) For unirradiated specimens, 3-5 specimens were tested. For irradiated specimens 2 specimens were tested.

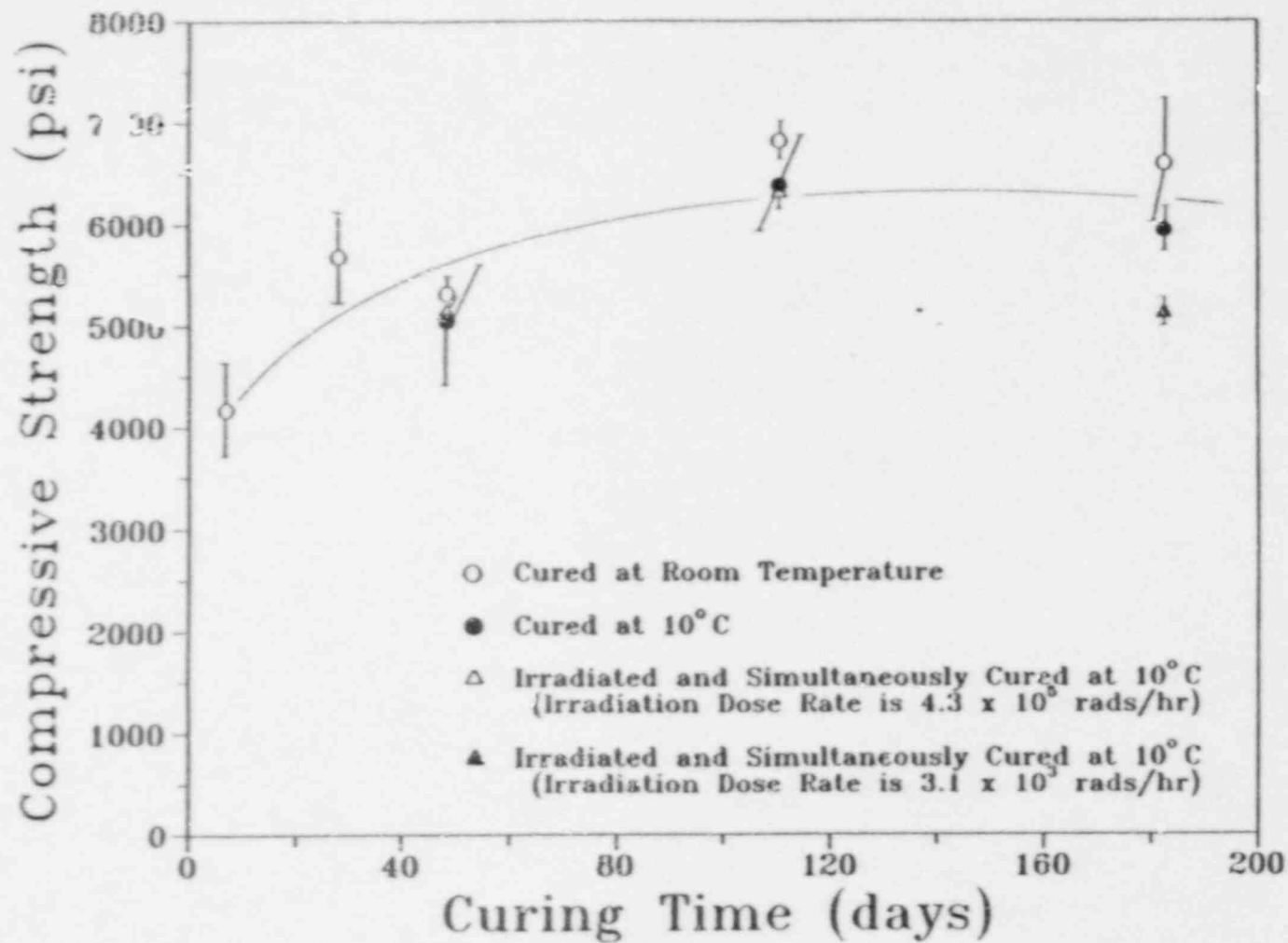


Figure 2.7 Compressive Strength of Portland I cement-mortar as a function of cure time and gamma irradiation.

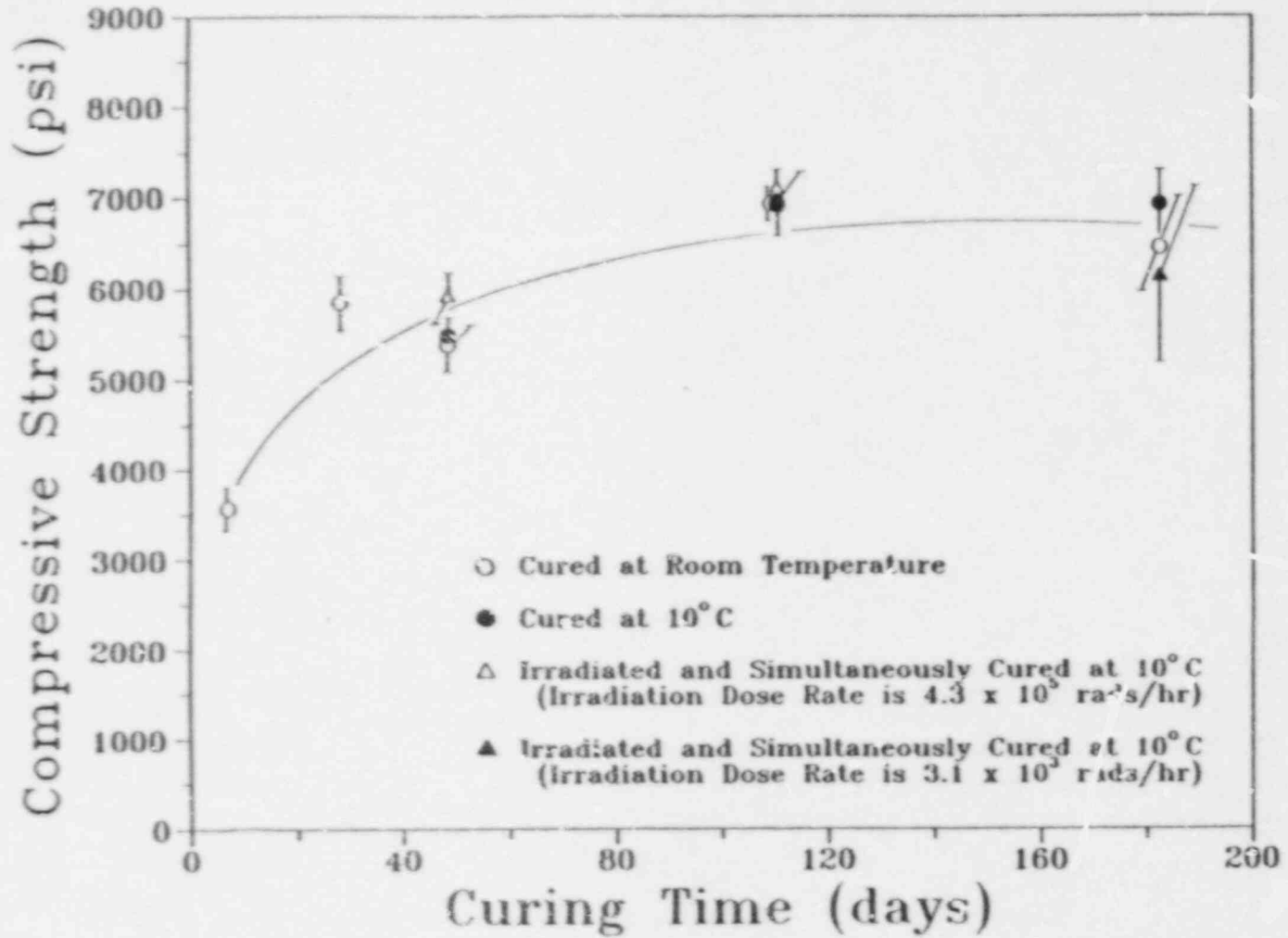


Figure 2.8 Compressive Strength of Portland V cement-mortar as a function of cure time and gamma irradiation.

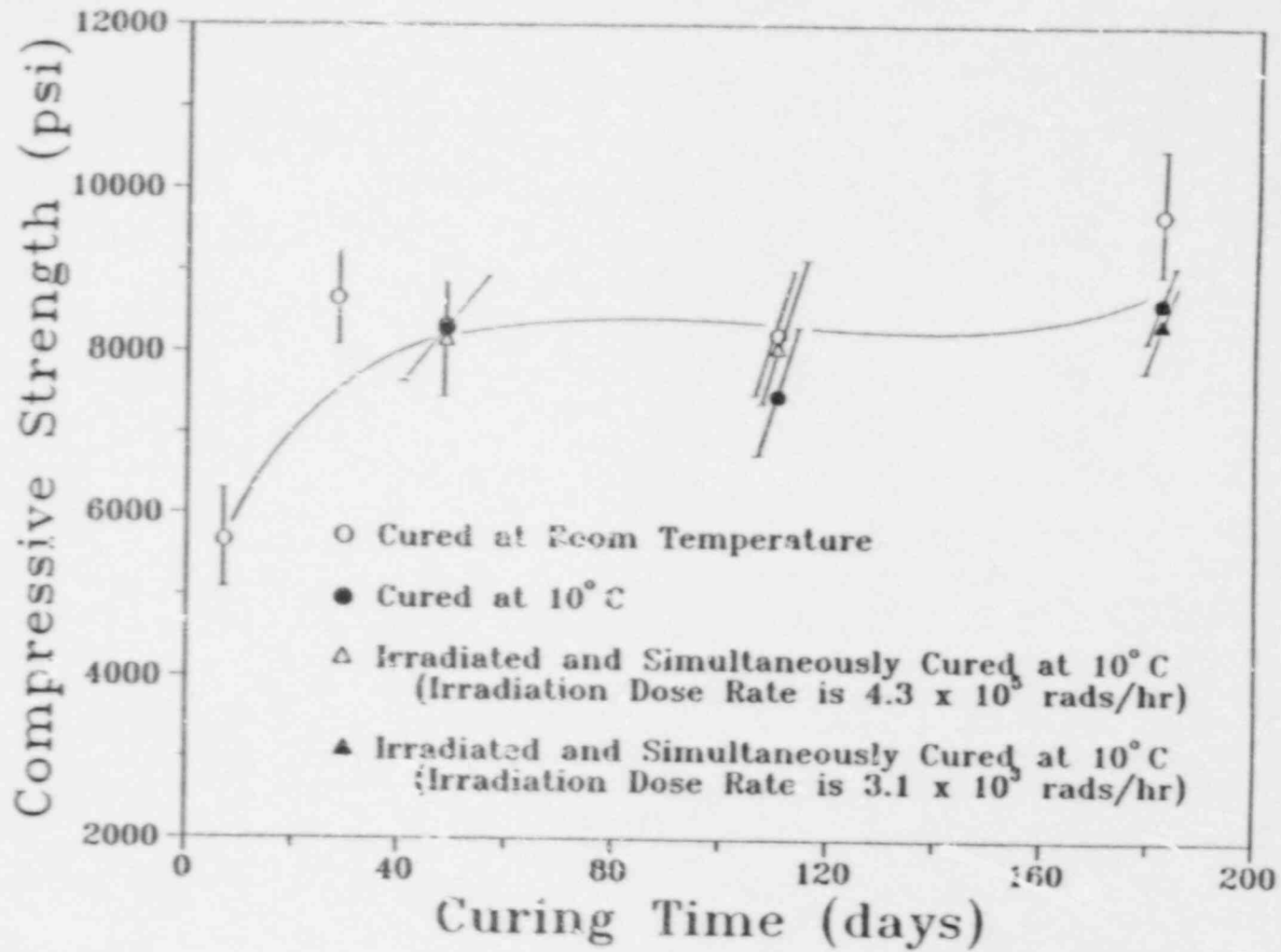


Figure 2.9 Compressive Strength of OHCM as a function of cure time and gamma irradiation.

3. DEGRADATION MECHANISMS IN HIGH-DENSITY POLYETHYLENE (HDPE)

3.1 Overview of Research Activities

High-density polyethylene is currently being used as a high-integrity container material for low-level wastes. Because of the need for such containers to maintain their structural integrity for at least 300 years (NRC Technical Position on Waste Form) potential failure/degradation modes must be determined for realistic environmental conditions. These include consideration of mechanical stress, gaseous/liquid environments within and external to the container, and the gamma radiation field. In some instances it is necessary to test under conditions more aggressive than those anticipated under shallow-land burial conditions so that failure or degradation modes can be more quickly identified and their relative importance assessed.

A combination of simple inexpensive tests (stressed U-bend samples) and more sophisticated uniaxial creep tests are being used to define the ranges of conditions for which mechanical failure/degradation is important. The test environments include Igepal CO-630, turbine oil and liquid scintillation fluid as well as air and deionized water (DIW), the control environments. Igepal CO-630 is a surfactant specified in standard ASTM tests for environmental stress cracking. Turbine oil is a possible constituent of low-level waste generated at reactor power plants, and is used in the current tests because of its known detrimental behavior to many types of plastic. Liquid scintillation fluids are not likely to be disposed of in burial sites at this time because of more stringent controls on their disposal. However, they are being evaluated here because they are representative of the class of organic solvents containing toluene and xylene. As such they will give valuable insights regarding a type of potential failure or degradation mode of HDPE.

In addition to the above-mentioned test environments, the effect of gamma irradiation on crack initiation and propagation in U-bend specimens is being studied. The samples are being irradiated in the BNL gamma irradiation test facility.

A description of the various subtasks is given below.

3.2 Crack Initiation and Propagation in a Gamma-Radiation Environment

Crack initiation and propagation is important in stressed HDPE containers because of the anticipated embrittlement by gamma irradiation. A simple inexpensive test was developed at BNL involving the use of static "U-bend" samples exposed to air and gamma radiation. Early tests were carried out on relatively large U-bends made by bending strips of HDPE measuring 25 x 2.5 x 0.32 cm (10" x 1" x 0.125") (Soo, and others, 1987). A more comprehensive set of tests was later initiated to obtain more detailed statistical data on crack initiation and propagation. These were on miniature U-bends manufactured from HDPE strips measuring 10.2 x 1.27 x 0.32 cm (4" x 0.5" x 0.125"). Holes were drilled at distances of 1.27 cm (0.5") from each end of the strips so that nuts and bolts could be used to hold the ends

of the strip together when the U-bends were made. The specimens were prepared with the outer surfaces of the U-bends in three different conditions:

- Type I - the as-received oxidized condition, which will have "natural" cracks present, as a result of bending,
- Type II - as above, but with 10 mils of the oxidized surface removed with emery paper prior to bending. No cracks were formed during bending,
- Type III - the as-received "non-oxidized" surface which also does not crack during bending.

Table 3.1 shows the test matrix for the U-bend irradiation tests.

Table 3.1 Test matrix for crack-propagation studies on irradiated Marlex CL-100 miniature U-bend specimens.

Gamma Dose Rate (rad/h)	Outer Surface Condition of U-Bend		
	Oxidized Surf. Present (Type I)	Oxidized Surf. Removed (Type II)	Non-Oxidized Surf. Present (Type III)
0	8 ⁽¹⁾	8	8
1.4 x 10 ³	8	8	8
8.4 x 10 ³	8	8	8
4.4 x 10 ⁵	8	8	8

(1) Number of specimens.

An examination of the irradiated specimens was made recently and is described in the last quarterly report (Soo, and others, 1988). It was shown that cracks could be initiated and be propagated in all three types of U-bend specimen. Cracking is most pronounced in Type I specimens, followed by Type III and then Type II. Cracks tend to initiate and propagate more readily in regions away from the apex regions of the specimens. This seems unusual since the apex regions are supposedly more highly stressed. It was postulated that stress relaxation caused by polymer chain scission may lead to a more rapid decrease in the high tensile stresses in the apex region (Soo, and others, 1988). This would help explain the slower rates of crack propagation.

3.3 Crack Initiation and Propagation in Chemical Environments

The above studies on irradiation-induced cracking show that embrittlement is associated with gamma-induced oxidation of the HDPE. In irradiation environments, where oxygen is at extremely low levels, cracking in U-bends is restricted (Adams and Soo, 1988). To evaluate more closely the effects of oxygen on cracking, a series of new U-bend tests was initiated in August, 1987. As was the case for the irradiated specimens, eight replicate U-bends were tested in air, deionized water, nitrogen and a vacuum. Only Type I specimen were studied. The test equipment consists of glass dessicators (without dessicant) with the lids sealed by vacuum grease. The air, nitrogen and water environments were maintained at atmospheric pressure at 20°C. The vacuum environment, unfortunately, was not maintained throughout the first test period which ended at the beginning of April. Thus, effects observed cannot be fully attributed to oxygen-free conditions.

The preparation of the specimens for the tests was similar to that for the irradiated U-bends with one important exception. For the current specimens the 10.2 x 1.27 x 0.32 cm (4" x 0.5" x 0.125") HDPE strips were not simply bent by hand and the two ends joined by a nut and bolt. It was decided to try to standardize a bend procedure such that excessive bending did not accidentally occur during specimen preparation. This involved gently bending the strip around a 1.27 cm (0.5 in.) metal rod and threading the bolt through the holes in the end sections. The nut and bolt were connected and the rod was removed to allow full tightening of the nut and bolt. The new procedure was found to produce less large cracks in the oxidized surfaces of the specimens, but numerous very small cracks were present. Figures 3.1 through 3.8 shows crack patterns in the U-bends sketched 24 h after bending, and again after 227 d exposure to the various environments. The numbers of large and small cracks are given in Table 3.2. A large crack is defined as being one with a length greater or equal to one-half of the U-bend width (i.e. 0.64 cm, 0.25 in.). A small crack is one measuring less than this size. It may be noted that despite care in bending the specimens, and their random allocations to batches of eight replicate samples, the numbers of starting cracks are not always similar for each batch. For example, the batch to be tested in nitrogen contained a total of 78 cracks whereas those to be exposed to a vacuum had 110 cracks. Nevertheless, the trends for a crack initiation and propagation show the following important features:

- a) The numbers of large and small cracks upon test initiation are approximately equal.
- b) The total numbers of cracks after test increase by about 30 percent for all environments.
- c) The percentages of large cracks increase much faster than those for small cracks, showing that small cracks grow readily to large size. For each small crack reaching the large crack status, a new small crack is usually initiated to replace it. Hence, there are approximately equal numbers of small cracks at the start and end of the test period.

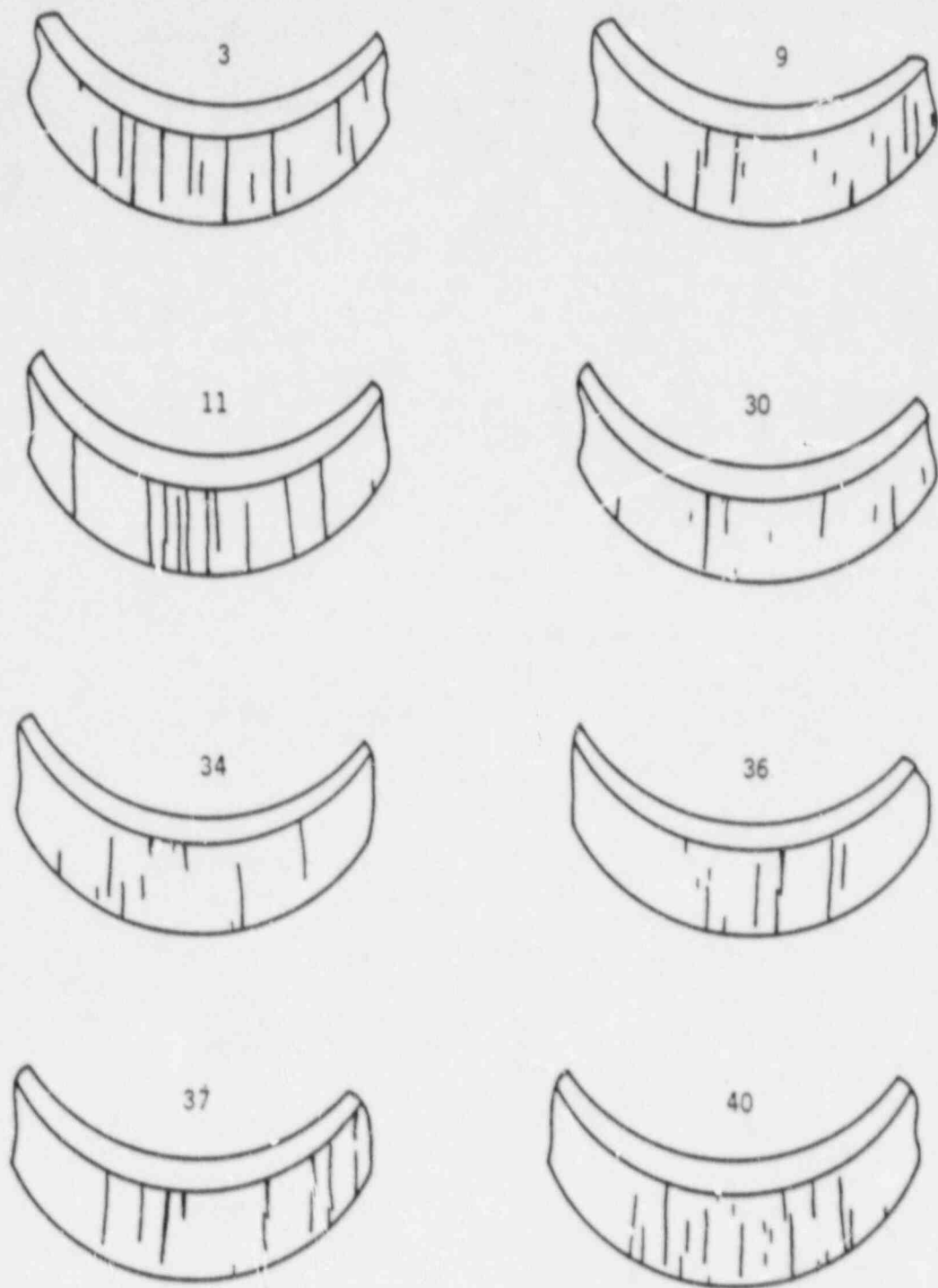


Figure 3.1 Crack patterns formed in the apex regions of Marlex CI-100 HDPE U-bend specimens prior to long-term exposure to air. Specimen numbers given above sketches.

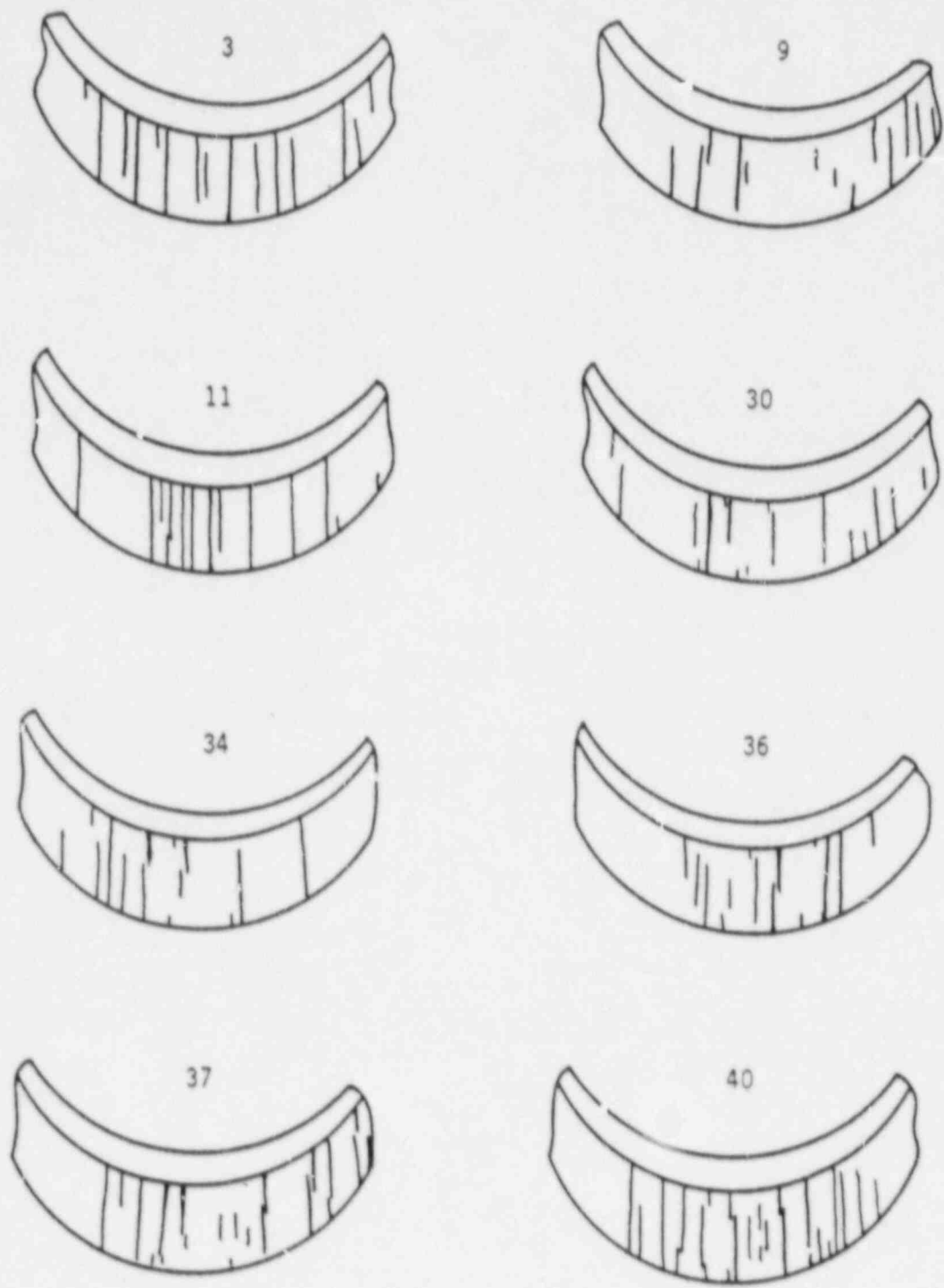


Figure 3.2 Crack patterns in the HDPE U-bend specimens shown in Figure 3.1 after 227 d exposure to air at 20 C. Specimen numbers given above sketches.

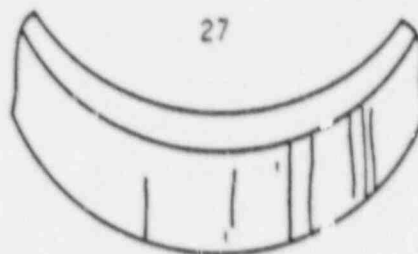
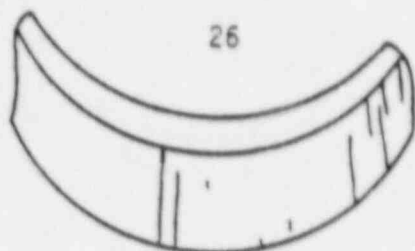
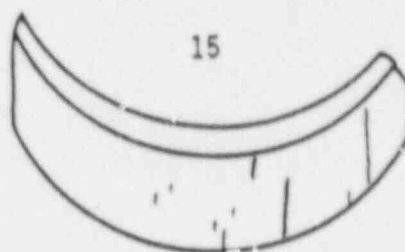
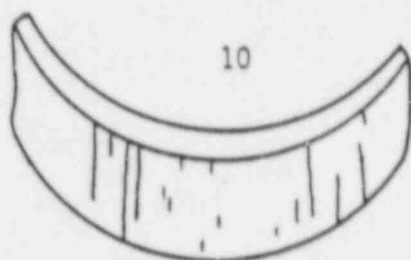
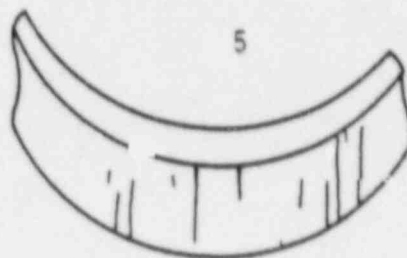
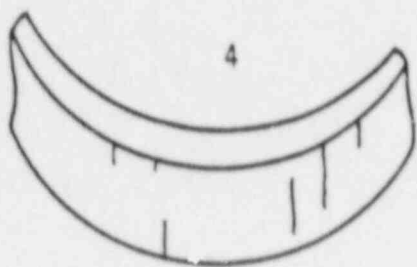
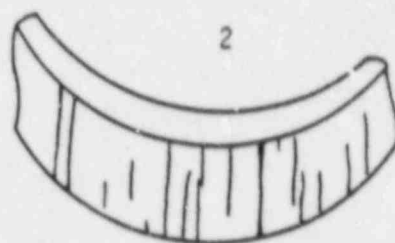
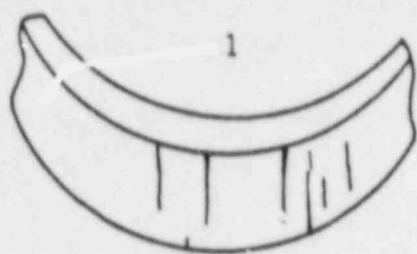


Figure 3.3 Crack patterns formed in the apex regions of Marlex CL-100 HDPE U-bend specimens prior to long-term exposure to deionized water. Specimen numbers given above sketches.

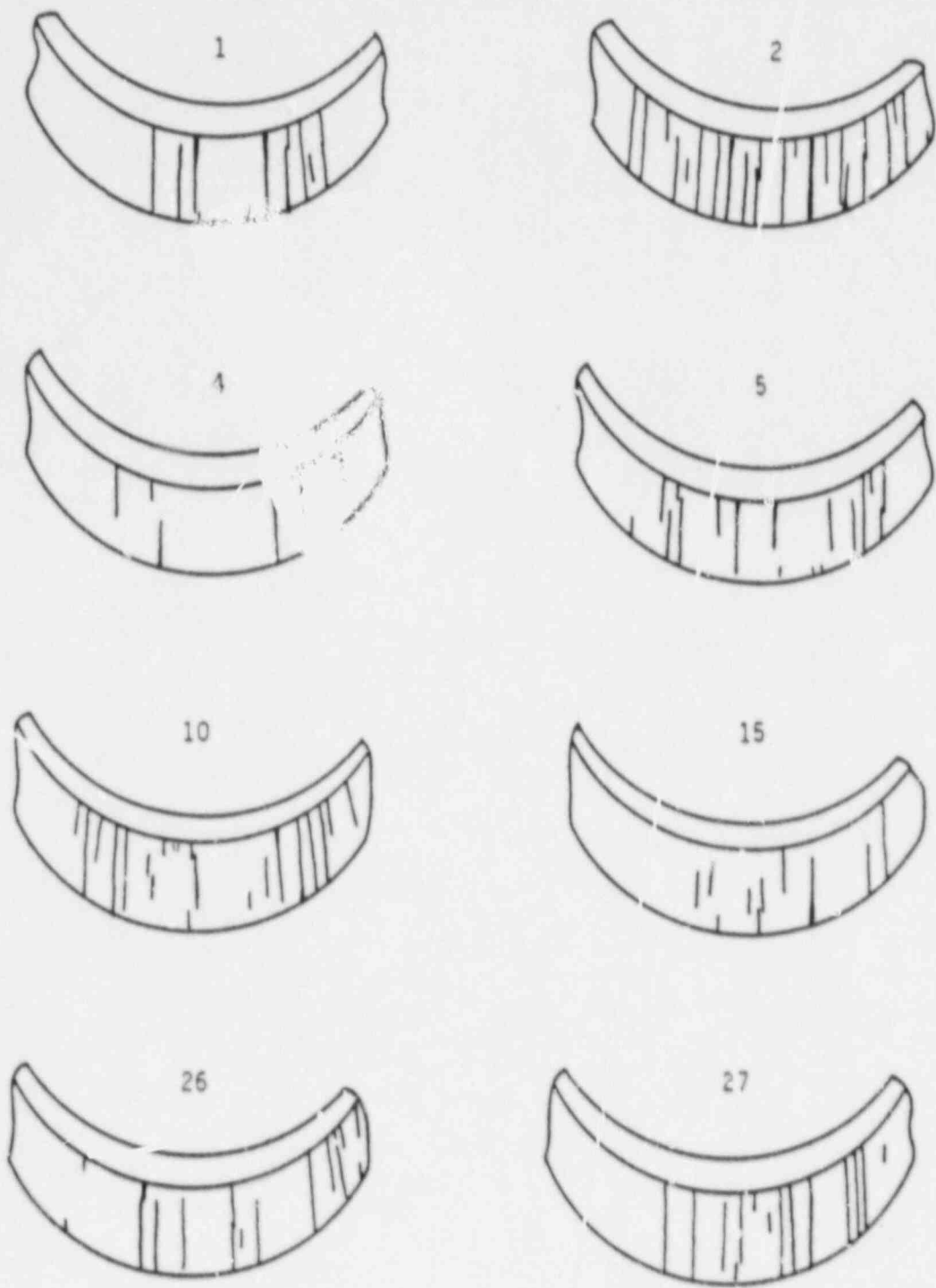


Figure 3.4 Crack patterns in the HDPE U-bend specimens shown in Figure 3.3 after 227 d exposure to deionized water at 20 C. Specimen numbers given above sketches.

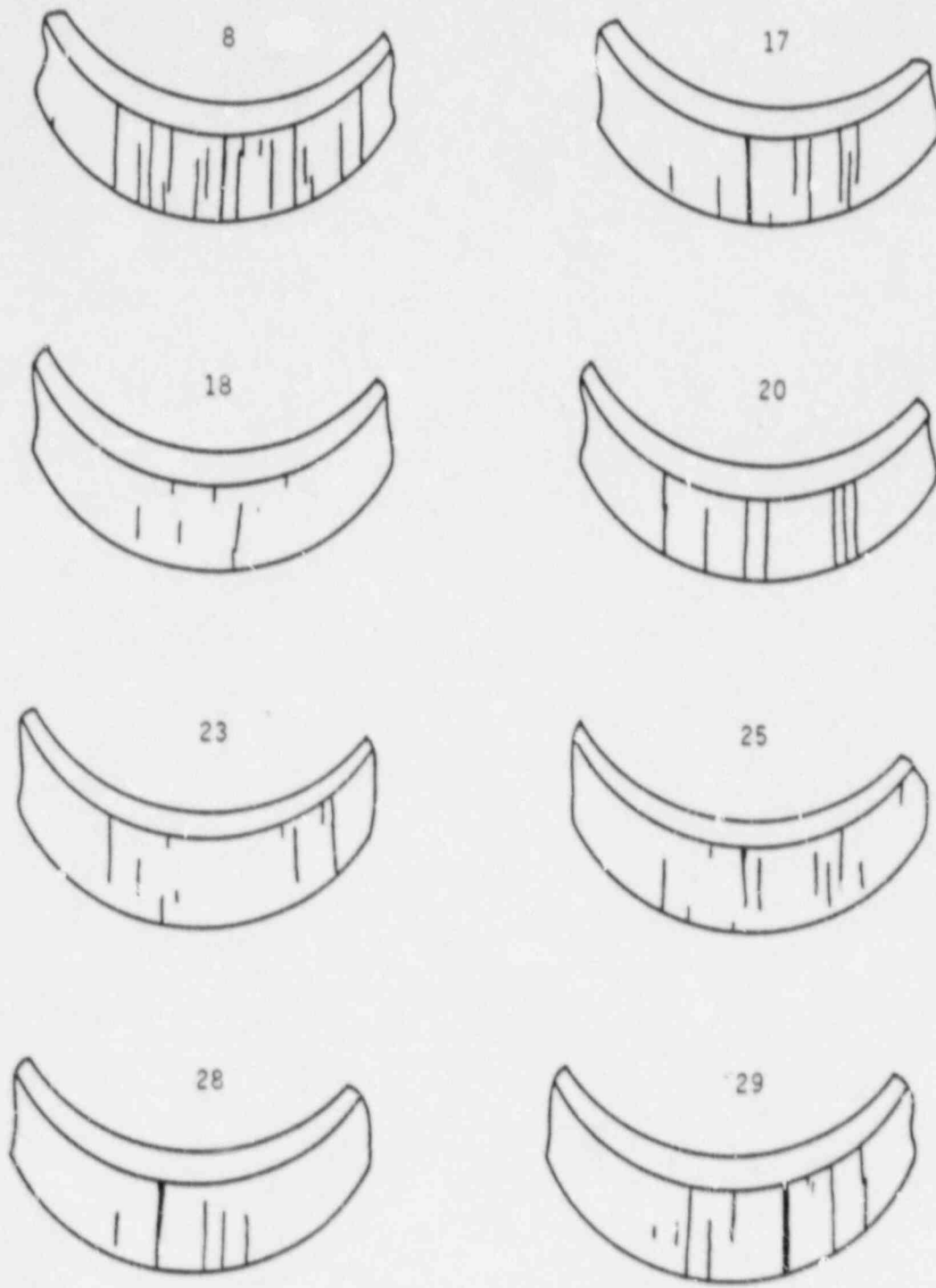


Figure 3.5 Crack patterns formed in the apex regions of Marlex CL-100 HDPE U-bend specimens prior to long-term exposure to nitrogen. Specimen numbers given above sketches.

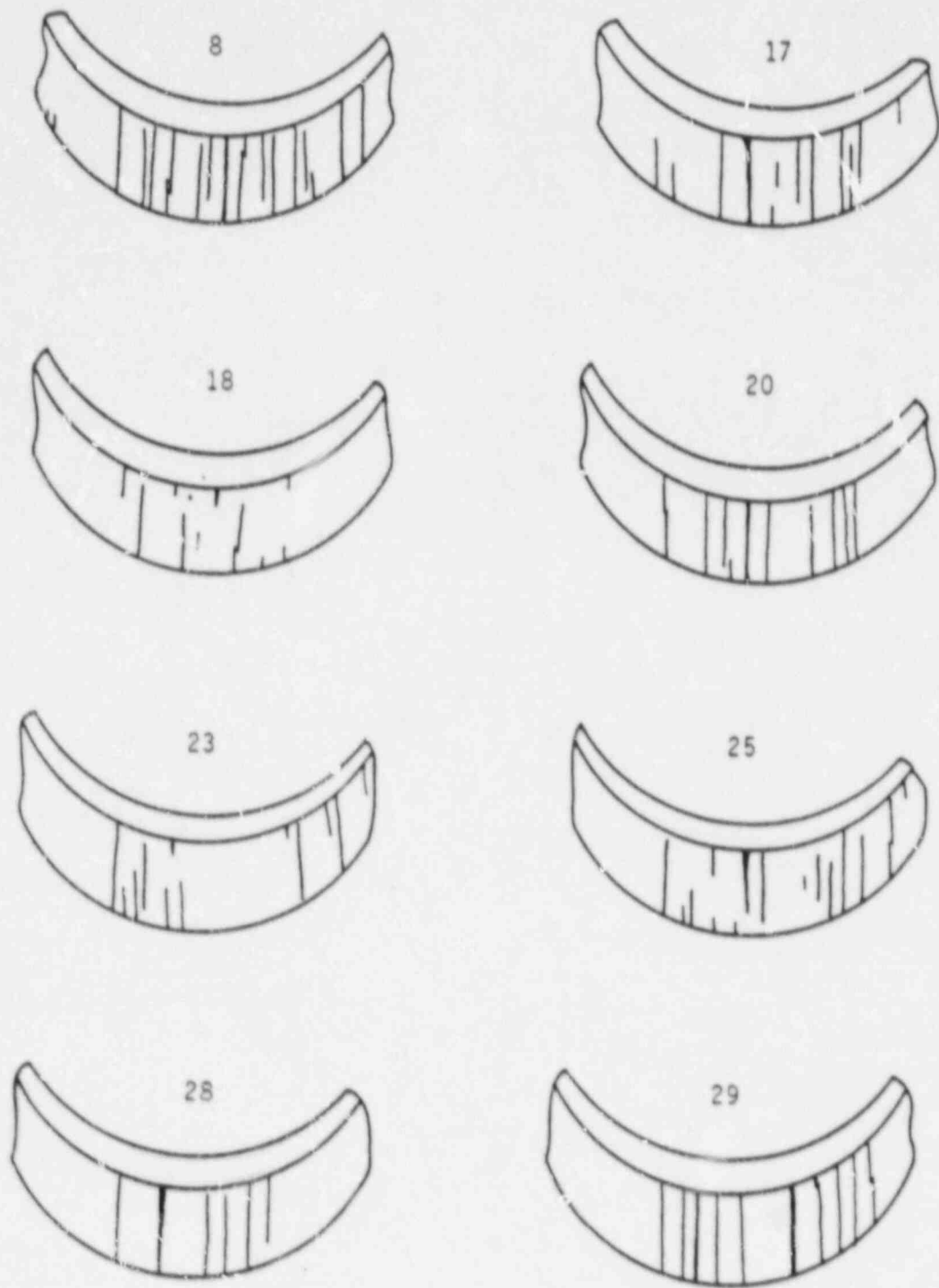


Figure 3.6 Crack patterns in the U-bond specimens shown in Figure 3.5 after 227 d exposure to nitrogen at 20 C. Specimen numbers given above sketches.

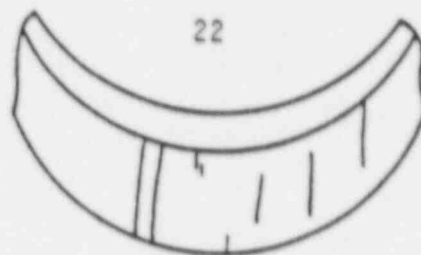
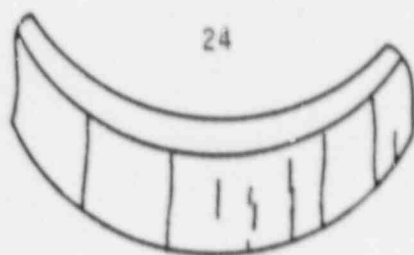
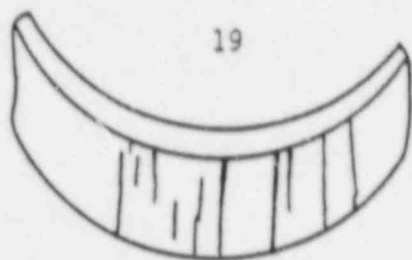
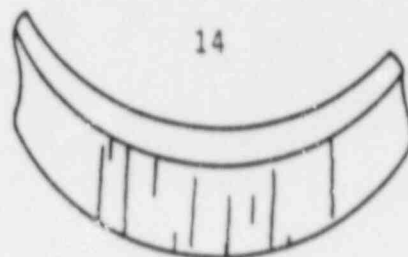
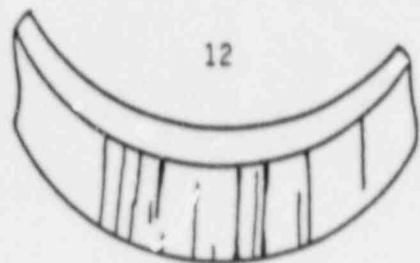
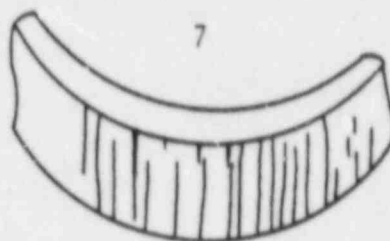
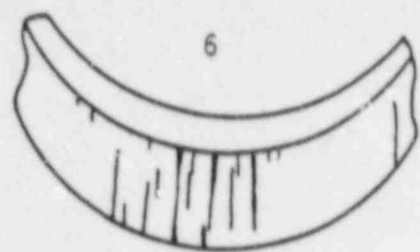


Figure 3.7 Crack patterns formed in the apex regions of Marlex CL-100 HDPE U-bend specimen prior to long-term exposure to a vacuum. Specimen numbers given above sketches.

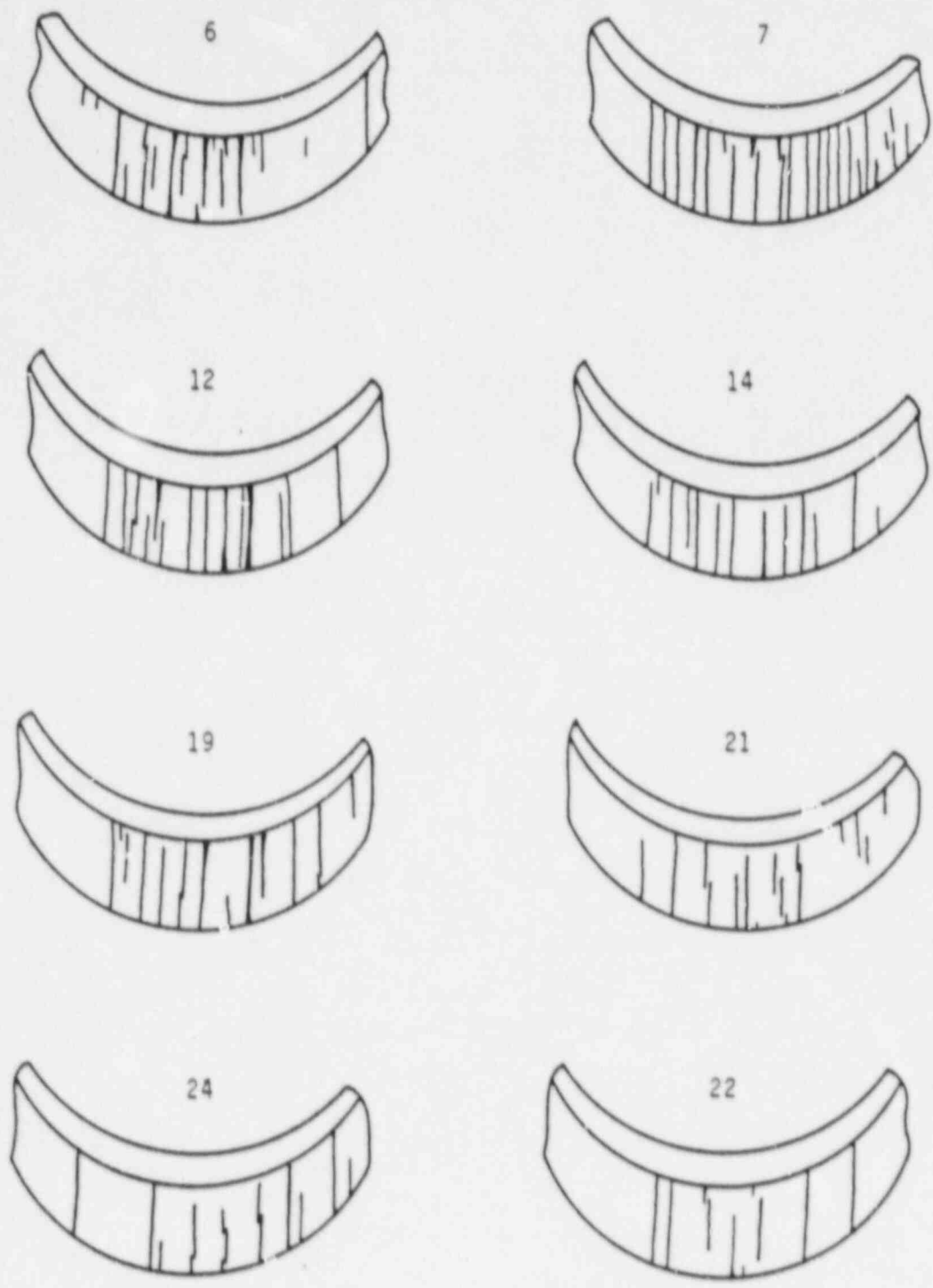


Figure 3.8 Crack patterns in the U-bend specimens shown in Figure 3.7 after 227 d exposure to initial vacuum conditions. Vacuum was lost through a slow leak during the test period. Specimen numbers given above sketches.

Table 3.2 Cracking in Type I HDPE U-bend specimens exposed for 227 d to various test environments.⁽¹⁾

Environment	Cracks Before Exposure			Cracks After Exposure			Percent Change in Numbers of Cracks		
	Large	Small	Total	Large	Small	Total	Large	Small	Total
Air	48	58	106	70	63	133	45.8	8.6	25.5
DIW	41	48	89	69	50	119	68.3	4.2	33.7
N ₂	44	34	78	63	36	99	43.2	5.9	26.9
Vacuum ⁽²⁾	58	52	110	80	46	146	37.9	-11.5	32.7

Notes:

1. The numbers of cracks are the totals counted for each batch of 8 replicate specimens.
2. Vacuum not maintained throughout test period.

Work by Adams and Soo (1988) proves that U-bend specimens irradiated in the presence of ion-exchange resins do not show crack initiation or crack propagation. Oxygen is effectively scavenged by the large volume of resin beads as a result of gamma-induced oxidation reactions. This prevents embrittlement of the HDPE by oxidation processes (Clough, 1981). Since cracking was noted in the four environments studied here, it is an indication that even small quantities of oxygen (in the nitrogen as a contaminant, or as a dissolved gas in water) can cause crack propagation in U-bend samples over long periods of time.

Work will continue on the U-bend samples and results will be given in a future report.

3.4 Uniaxial Creep Behavior

The tests on HDPE creep in the various environments are proceeding. Since the emphasis is now on long-term creep behavior (low stress levels) failure of specimens is becoming increasingly rare. In fact, none of the 15 ongoing tests reported in the last progress report failed during this quarter (Soo, and others, 1988). Tables 3.3 and 3.4 summarize creep data from past and ongoing tests.

A series of new tests was prepared this quarter to quantify creep under the conjoint action of stress and gamma irradiation. Seemingly contradictory behavior was found in two prior BNL studies. One by Dougherty (1984) showed that irradiation enhanced the rate of creep compared to similarly stressed unirradiated material; the other study showed the reverse (Soo, and others, 1986). It was postulated that the two sets of results could be rationalized on the basis that Dougherty's results were for high stress, lower dose rate conditions, and those by Soo were for lower stresses at higher dose rates. The work in the current irradiation-creep program is designed to examine this hypothesis. Table 3.5 is a test matrix for this work. The HDPE to be used is from an original BNL batch, which was used in the two earlier studies.

The four creep tests under non-irradiation conditions have been completed. Work on the irradiation-creep tests will be initiated next quarter, after the creep apparatus has been assembled and dosimetry work completed so that the specimens can be located in the correct dose rate locations.

3.5 Testing Protocol for HDPE

The useful lifetime for a HDPE waste container will normally depend on many variables, including the level of stress, the irradiation dose rate, the internal chemical and irradiation environment determined by the waste composition, and the external environment determined by the burial conditions. These conditions may change with time so the estimation of failure times for container is extremely difficult.

To develop an approach to determining container performance requires consideration of several factors, which include the following:

Table 3.3 Creep test data for Marlex CL-100 HDPE tested in air and deionized water at room temperature.

Test Number	Specimen Condition	Test Environment	Stress		Failure Time (h)	Elong. at Break (%)
			(MPa)	(psi)		
381	As rec.	Air	13.79	2000	4.0	56.0
382	As rec.	Air	13.79	2000	0.98	56.6
367	As rec.	Air	13.10	1900	6.8	56.8
369	As rec.	Air	13.10	1900	5.8	46.6
374	As rec.	Air	12.76	1850	5.4	46.2
365	As rec.	Air	12.41	1800	41.0	74.6
359	As rec.	Air	12.41	1800	11.3	>33.6
366	As rec.	Air	12.10	1750	52.5	76.0
362	As rec.	Air	12.00	1740	28.5	>49.0
358	As rec.	Air	11.72	1700	80.3	79.6
361	As rec.	Air	11.03	1600	457	79.7
360	As rec.	Air	10.86	1575	212	85.4
350(a)	As rec.	Air	10.62	1540	166	72.9
350(b)	As rec.	Air	10.62	1540	502	55.0
300	As rec.	Air	10.34	1500	662	61.6
315	As rec.	Air	10.34	1500	761	58.2
363	As rec.	Air	10.17	1475	4023	60.4
357	As rec.	Air	10.00	1450	3821	55.1
380	As rec.	Air	10.00	1450	2455	66.8
377	As rec.	Air	9.83	1425	5173	53.5
316	As rec.	Air	9.65	1400	5378	36.6
364	As rec.	Air	9.31	1350	1819	71.9
391	As rec.	Air	9.13	1325	Ongoing	-
355	As rec.	Air	8.96	1300	3100	37.0
390	As rec.	Air	8.96	1300	Ongoing	-
321	As rec.	Air	8.27	1200	7740	16.2
388	As rec.	Air	7.93	1150	Ongoing	-
322	As rec.	Air	7.24	1050	Ongoing	-
384	Old HDPE	Air	13.79	2000	1.8	67.6
358	Old HDPE	Air	13.10	1900	5.3	46.6
375	Old HDPE	Air	12.76	1850	18.6	(3)
351	Old HDPE	Air	12.58	1825	5.8	82
344	Old HDPE	Air	11.72	1700	47	121.6
343	Old HDPE	Air	11.03	1600	127	80.0
342	Old HDPE	Air	10.34	1500	2544	96.3
317	Old HDPE	Air	10.34	1500	7514	69.2
318	Old HDPE	Air	9.65	1400	Ongoing	-
386	Old HDPE	Air	8.27	1200	Ongoing	-
387	(1)	Air	13.79	2000	Ongoing	-
385	(1)	Air	12.41	1800	Ongoing	-
338	(1)	Air	11.03	1600	2319	585
323	(1)	Air	10.34	1500	7704	248.9
320	(1)	Air	8.27	1200	Ongoing	-
337	As rec.	DIW	11.03	1600	112	58.6
347	As rec.	DIW	10.69	1550	57	54.6
301	As rec.	DIW	10.34	1500	2027	95.5
302	As rec.	DIW	9.65	1400	5854	54.5
334	As rec.	DIW	8.27	1200	Ongoing	-
339	(1)	DIW	11.03	1600	200	221.6
327	(1)	DIW	10.34	1500	452	85.2
326	(1)	DIW	8.27	1200	Ongoing	-
306	(2)	DIW	10.34	1500	1154	57.5
310	(2)	DIW	9.65	1400	6264	53.5

NOTES:

1. 10 mils removed from oxidized surface of specimen.
2. 10 mils removed from non-oxidized surface of specimen.
3. LVDT faulty; elongation not accurately known.

Table 3.4 Creep test data for Marlex CL-100 HDPE tested in various environments at room temperature.

Test Number	Specimen Condition	Test Environment	Stress		Failure Time (h)	Elong. at Break (%)	Weight Change (% per test day)
			(MPa)	(psi)			
370	As rec.	Oil	11.03	1600	45.9	92.1	0.19
305	As rec.	Oil	10.34	1500	128	60.3	0.06
345	As rec.	Oil	8.96	1300	102	43.4	0.02
348	As rec.	Oil	8.96	1300	168	51.1	0.04
352	As rec.	Oil	8.62	1250	198	84.1	0.01
325	As rec.	Oil	8.27	1200	1502	36.3	-
396	As rec.	LSF	12.41	1800	7.9	85.0	0.72
379	As rec.	LSF	11.72	1700	9.6	94.8	-
378	As rec.	LSF	11.38	1650	10.5	49.3	1.47
395	As rec.	LSF	11.03	1600	33.1	89.9	0.34
308	As rec.	LSF	10.34	1500	14	83.5	0.25
309	As rec.	LSF	9.65	1400	35	98.0	0.15
341	As rec.	LSF	8.27	1200	50	98.5	1.40
333	As rec.	LSF	7.24	1050	340	95.8	0.02
383	As rec.	LSF	6.89	1000	1602	80.6	-
394	As rec.	LSF	6.72	975	Ongoing	-	-
330	(1)	LSF	9.65	1400	29	76.0	-
332	(1)	LSF	8.27	1200	85	216.0	-
331	(1)	LSF	7.24	1050	Ongoing	-	-
313	(2)	LSF	10.34	1500	12	55.0	0.28
311	(2)	LSF	9.65	1400	31	77.0	0.21
42	Old HDPE	LSF	10.34	1500	12	86.1	-
55	Old HDPE	LSF	9.65	1400	35	37.8	-
62	Old HDPE	LSF	8.27	1200	200	100.7	-
392	As rec.	Igepal	12.41	1800	3.1	52.3	0.27
393	As rec.	Igepal	11.72	1700	17.7	51.8	0.23
371	As rec.	Igepal	11.03	1600	45.6	54.7	0.13
303	As rec.	Igepal	10.34	1500	65	49.1	0.06
304	As rec.	Igepal	9.65	1400	106	54.8	0.03
346	As rec.	Igepal	8.96	1300	128	47.3	0.02
324	As rec.	Igepal	8.27	1200	1194	22.0	-
389	As rec.	Igepal	8.10	1175	Ongoing	-	-
106	Old HDPE	Igepal	12.41	1800	8	74.8	-
105	Old HDPE	Igepal	12.41	1800	9	69.2	-
107	Old HDPE	Igepal	11.72	1700	50	87.4	-
108	Old HDPE	Igepal	11.72	1700	47	54.6	-
72	Old HDPE	Igepal	10.34	1500	216	68.7	-
113	Old HDPE	Igepal	10.34	1500	366	62.2	-
114	Old HDPE	Igepal	10.34	1500	372	79.2	-
84	Old HDPE	Igepal	10.34	1500	95	115.3	-
340	(1)	Igepal	10.34	1500	312	97.3	0.04
329	(1)	Igepal	9.65	1400	476	59.4	-
328	(1)	Igepal	8.27	1200	Ongoing	-	-
314	(2)	Igepal	10.34	1500	56	71.4	0.09
312	(2)	Igepal	9.65	1400	106	50.4	0.03

NOTES:

1. 10 mils removed from oxidized surface of specimen.
2. 10 mils removed from non-oxidized surface of specimen.

Table 3.5 Irradiation-creep test matrix for HDPE

Test Medium	Stress		γ Flux (rad/h)
	(MPa)	(psi)	
Air	12.58	1825	0
Air	12.58	1825	5×10^3
Air	12.58	1825	3×10^4
Air	11.72	1700	0
Air	11.72	1700	5×10^3
Air	11.72	1700	3×10^4
Air	11.07	1600	0
Air	11.07	1600	5×10^3
Air	11.07	1600	3×10^4
Air	10.34	1500	0
Air	10.34	1500	5×10^3
Air	10.34	1500	3×10^4

- a) A specification of all possible material degradation modes which could lead to eventual failure in the service environment. Lack of identification of a failure or degradation mode will preclude the development of a strategy to eliminate its occurrence, or reduce its impact, within the design lifetime.
- b) Performance of experiments to characterize the individual failure modes under prototypic and accelerating conditions. Accelerating conditions are useful in that they allow a degradation/failure mode to be observed and quantified within practical testing periods. Through a knowledge of the fundamental mechanism responsible it may be possible to fit the data from accelerated tests to a theoretical expression which may then be used to predict long-term performance. In the absence of a sound theoretical knowledge of the mechanism, an empirical expression could be used and this also could be used to estimate failure times for prototypic environments despite the greater uncertainty in the prediction.

An example of a useful empirical equation to predict lifetime may be found in studies of carbon steel corrosion in soils (Kempf, and others, 1987). Using pitting corrosion data from Romanoff (1957) it was shown that the maximum pit depth could be given by:

$$d_m = 29 t^{0.39}$$

in which d_m is the depth in mils and t is the corrosion time in years. Such an expression will allow an estimation to be made of the maximum depth of attack so that the thickness of the steel component being designed for in-soil service can be sized to avoid penetration during the design lifetime.

- c) The use of experiments specified in (b), above, may identify conditions for which a particular failure mode ceases to exist. For example, there are instances for which the stress on a material becomes too low for stress-assisted cracking to occur. With this in mind, stress-corrosion and fatigue are often avoided by ensuring that the maximum service stress in the component being designed is significantly lower than the threshold stress required to cause failure. An important goal in designing a HDPE waste container should, then, be the adjustment of the design parameters and environmental conditions in such ways that the container becomes immune to as many potential failure modes as possible. The remaining failure modes must then be addressed by obtaining data from accelerated tests, as described above or, if available, from long-term prototypic in-service evaluations on the material of interest.

The work being undertaken in this area (Task 5) will address all of the three items described above. Specifically, failure/degradation modes for HDPE will be identified for conditions which may exist during the pre- and post-disposal periods. If required, testing protocols will be defined to supplement those that currently exist in the literature. The test data that are obtainable from such tests will be discussed with respect to their use in container design, and suggestions will be made on ways to minimize, or eliminate, the occurrence of specific failure or degradation modes in HDPE.

At the present time the following degradation/failure modes have been identified either from the literature or from research carried out in the current program.

a) Environmental Stress-Cracking

This involves the conjoint action of a tensile stress and a susceptible environment. The environment may provide a chemical (corrosive) effect or it may simply involve a non-reactive surface wetting phenomenon which accelerates crack propagation and failure (Shanahan; 1979, 1980). HDPE is usually very resistant to corrosion but under some conditions it may be slowly

dissolved (e.g. by toluene and xylene) so some form of chemical reaction could be involved. Igepal CO-630, nonylphenoxy poly (ethylenoxy) ethanol, is an ASTM-specified liquid for evaluating the susceptibility of HDPE to environmental stress-crack (see ASTM Standard D-2552). It is stated to be non-reactive and probably it acts as a simple surface wetting agent. On the other hand, BNL creep tests in scintillation fluid (see Table 3.4) show that the specimens have a relatively rapid rate of absorption of this fluid during test, which could indicate the presence of a chemical reaction with the HDPE. Therefore, a distinction should be made between non-reactive and reactive environments in the evaluation of environmental stress-cracking. Failure times as well as weight changes during test should be carried out to distinguish between the various environmental effects, if possible.

b) Irradiation Embrittlement

The U-bend tests in gamma-radiation environments show that crack initiation and fast propagation may occur if oxygen is present. Intermediate dose rates and intermediate stress levels are more likely to cause failure (Soo, and others, 1988). The mechanism is associated with bond cleavage which produces free radicals, which react with oxygen by a chain mechanism to form oxidation products that include hydroperoxides (Clough, 1981). As a consequence of these gamma-induced reactions, polymer chain scission and crosslinking occur.

Tests to characterize cracking may include static U-bend tests, such as those used in the current study, or more sophisticated stress-relaxation tests for which a load cell is used to monitor the stress level in the HDPE throughout the radiation period when cracking is occurring. Fracture mechanics techniques can also be used to investigate cracking as a function of stress intensity level and dose rate.

c) Ductile Failure

The usual type of ductile failure involves deformation at relatively high stress levels, such as those encountered during short-term tensile testing at a constant strain rate (e.g., ASTM D-638, Test for Tensile Properties of Plastics) or high stress creep behavior under a constant load (e.g., ASTM D-2990, Tensile, Compressive, and Flexural Creep and Creep-Rupture of Plastics). In many cases the HDPE test material is prepared by the melting of polyethylene resin which is molded or fabricated to a specific shape (sheet, drum, pipe, etc.). Normally, the fabrication process is carried out in air, and this results in the formation of an oxidized surface layer which has inferior ductility compared to underlying bulk material (Terselius, 1982).

In BNL tests this surface-oxidized material cracks after about 20 percent elongation, and subsequent deformation tends to concentrate in the cracked areas, eventually giving rise to failure in one of these regions. If the oxidized layer is mechanically removed prior to creep testing then deformation occurs more uniformly throughout the gage length of the specimen and "superplastic" type behavior often occurs. Table 3.3 shows that a non-oxidized creep specimen (#338) had an elongation-at-failure of 585 percent after creeping under a stress of 11.03 MPa (1600 psi). Specimen 361, which had an intact oxidized surface, had an elongation of only 79.7 percent at the same stress level. Clearly, both failures are ductile but oxidation-free HDPE has extraordinary ductility and will be far more resistant to failure at a given creep stress.

One may, therefore, specify two ductile failure modes: (i) ductile failure initiated at cracks in surface oxidized HDPE and (ii) superplastic failure in non-oxidized material.

d) Low-Stress Creep Embrittlement

The data in Figure 3.9 show ductilities at failure for creep tests carried out in air, deionized water, Igepal CO-630, turbine oil and scintillation fluid, as a function of stress. For air, water, oil, and Igepal it is seen the ductilities are tending to low values as the stress is decreased below 8.27 MPa (1100 psi). Liquid scintillation fluid also causes a drop in ductility in the low stress range, but the data are insufficient to show this convincingly. Clearly, at low stresses, embrittlement occurs under creep conditions. Failure, based on work in this program, is caused by the propagation of cracks which are nucleated in the oxidized surface material. Since deformation occurs most easily in these cracked regions it results in failure at low ductility. Other work by Graube (1976) on internally-pressurized HDPE pipes shows similar brittle failure at low pressures.

e) Impact Embrittlement

Low-temperature impact testing of a material measures the resistance of a material to failure from a high velocity impact. Calibrated machines are used to measure the energy absorbed by a stationary sample as a heavy load falls under gravity to impact and fracture it. This type of failure mode is not likely to be of importance with respect to container service conditions unless, for example, a HDPE container is embrittled by irradiation and fast loading from earth movement is encountered. However, the test is specified here because of its importance as a measure of the quality of polyethylene manufactured by industry (Philips Chem. Co., 1982). Such testing warrants serious consideration as a quality control test for HDPE containers.

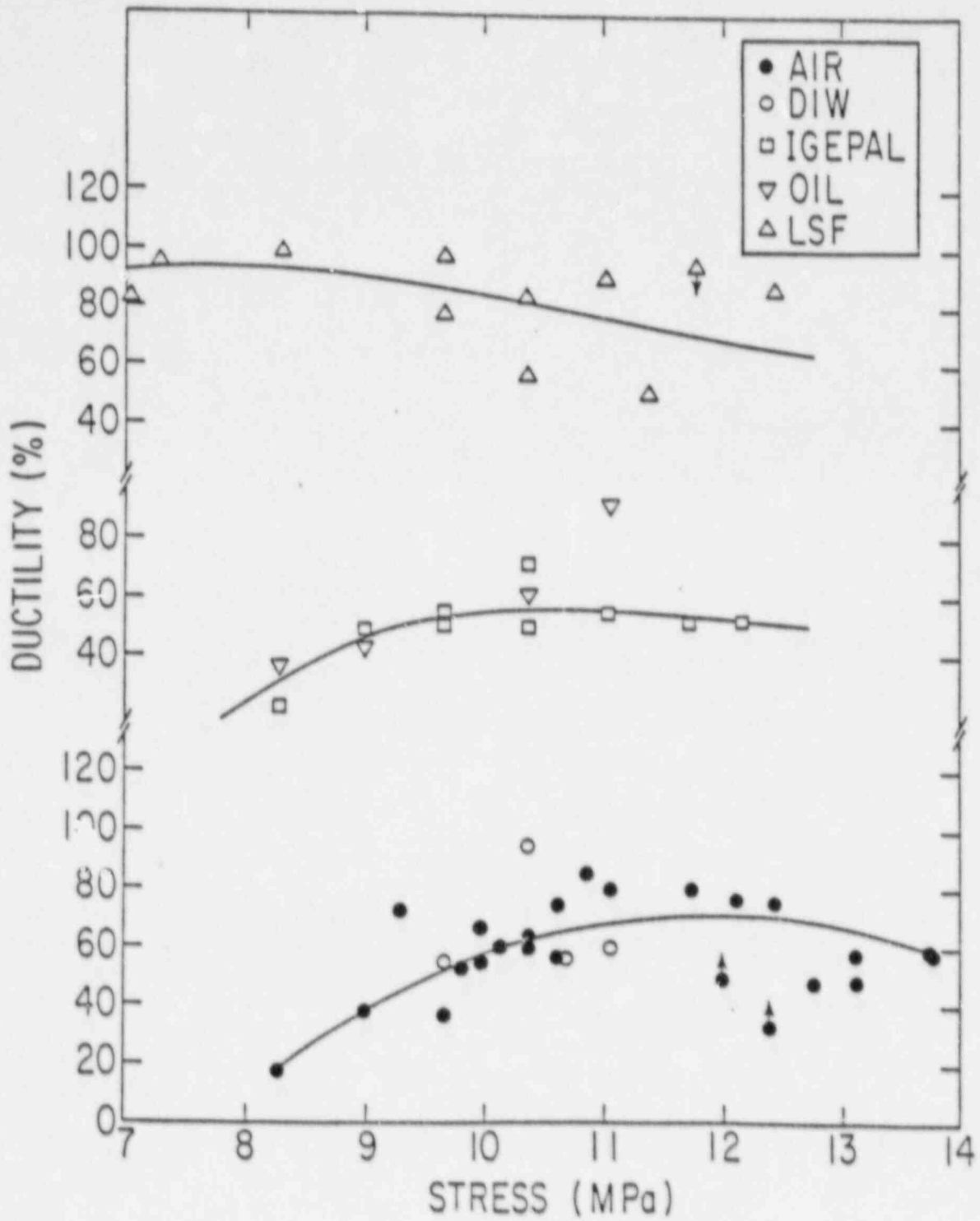


Figure 3.9 Elongations at failure for Marlex CL-100 HDPE tested at 20°C in various environments.

3.6 Publications on HDPE Research

A paper summarizing some of the salient aspects of the HDPE research effort was presented at Waste Management '88 in Tucson in February. Appendix I is a copy of the paper to be published in the proceedings.

4. BIODEGRADATION OF ION-EXCHANGE MEDIA

The typical report for this completed study has been typed and is undergoing internal quality assurance review.

A copy of a paper presented at Waste Management '88 is given in Appendix II.

5. REFERENCES

- Adams, J. W., and P. Soo, "The Impact of LWR Decontaminations on Solidification, Waste Disposal and Associated Occupational Exposure," NUREG/CR-3444, BNL-NUREG-51699, Vol. 5, (1988).
- Clough, R. L., and K. T. Gillen, "Combined Environmental Aging Effects: Radiation-Thermal Degradation of Polyvinylchloride and Polyethylene," J. Polymer Sci., Polymer Chemistry Edition, 19, 2041, (1981).
- Dougherty, D. R., and others, "An Evaluation of the Effects of Gamma Irradiation on the Mechanical Properties of High Density Polyethylene," NUREG/CR-3898, BNL-NUREG-51802, (1984).
- Graube, E., and others, "Thermoplastic pipes: experience of 20 years of creep rupture testing," Kurststoffe, 66, 2, (1976).
- Kalousek, G. L., and others, "Past, Present, and Potential Developments of Sulfate-Resisting Concretes," J. Testing and Evaluation, 4, 347, (1976).
- Kempf, C. R., and others, "Low-Level Waste Source Term Evaluation," Quarterly Progress Report, January-March 1987, WM-3276-2, June (1987).
- Philips Chem. Co., "Quality Control Tests for Crosslinking of Marlex CL-100 and CL-50," Philips Chemical Co., Bartlesville, OK 74004, Tech. Service Memorandum TSM-291, (1982).
- Romanoff, M., "Underground Corrosion," NBS Circular 579, (1957).
- Shanahan, M. E. R., and J. Schultz, "Environmental Stress Cracking of Polyethylene: Criteria for Liquid Efficiency," J. Polymer Sci., 17, 705 (1979).
- Shanahan, M. E. R., and J. Schultz, "Correlation Between Environmental Stress Cracking and Liquid Sorption for Low-Swelling Liquids," J. Polymer Sci., 18, 19 (1980).
- Soo, P., and others, "Low-Level Waste Package and Engineered Barrier Study," Quarterly Progress Report, July-September 1987, WM-3291-5, December (1987).
- Soo, P., and others, "Low-Level Waste Package and Engineered Barrier Study," Quarterly Progress Report, October-December 1987, WM-3291-6, April (1988).
- Soo, P., and others, "The Effects of Environment and Gamma Irradiation on the Mechanical Properties of High Density Polyethylene," NUREG/CR-4607, BNL-NUREG-51991, (1986).
- Terselius, B., V. W. Gedde, and J. F. Jansson, "Structure and Morphology of Thermally Oxidized High Density Polyethylene Pipe," Polymer Eng. and Sci., 22, 422, (1982).

APPENDIX I

EFFECTS OF CHEMICAL AND GAMMA IRRADIATION ENVIRONMENTS ON THE
MECHANICAL PROPERTIES OF HIGH-DENSITY POLYETHYLENE (HDPE)

P. Soo
Brookhaven National Laboratory,
Upton, New York 11973

INTRODUCTION

High-density polyethylene (HDPE) is currently being used as a high-integrity container material for low-level wastes. Because of the need for such containers to maintain their structural integrity for at least 300 years (NRC Technical Position on Waste Form) potential failure/degradation modes must be determined for realistic environmental conditions. These include consideration of mechanical stress, gaseous/liquid environments within and external to the container, and the gamma radiation field.

In some instances it is necessary to test under conditions more aggressive than those anticipated under shallow-land burial conditions so that failure or degradation modes can be more quickly identified and their relative importance assessed.

A combination of simple inexpensive tests (stressed U-bend samples) and more sophisticated longer-term uniaxial creep tests are being used to define the ranges of conditions for which mechanical failure/degradation is important. The test environments include Igepal CO-630, turbine oil and liquid scintillation fluid as well as air and deionized water, the control environments. Igepal CO-630 is a surfactant specified in standard ASTM tests for environmental stress cracking. Turbine oil is a possible constituent of low-level waste generated at reactor power plants, and is used in the current tests because of its known detrimental behavior to many types of plastic. Liquid scintillation fluids are not likely to be disposed of in burial sites at this time because of more stringent controls on their disposal. However, they are being evaluated here because they are representative of the class of organic solvents containing toluene and xylene. As such they will give valuable insights regarding a type of potential failure or degradation mode for HDPE.

In addition to the above-mentioned test environments, the effect of gamma irradiation on crack initiation and propagation is being studied. A description of the work is given below.

Material

The material used in this study was made from Marlex CL-100 (a highly cross-linked HDPE, trademark of the Philips Chemical Co.). The powder was used to rotationally mold a 5000-L drum by Poly-Processing, Inc., Monroe, LA. Test specimens were cut or stamped from the 3.18 mm (0.125 in.) thick walls of the drum. Owing to the molding procedure, the internal surfaces of the drum

were oxidized by air during the high temperature molding process, whereas the outer surfaces, being in contact with the mold, were not. Since the oxidized surface is more brittle, it tends to crack more easily during deformation and, as will be shown below, this could lead to shorter failure times when compared to non-oxidized HDPE.

Crack Initiation and Propagation in a Gamma-Radiation Environment

Crack initiation and propagation could be important in stressed HDPE containers because of the anticipated embrittlement by gamma irradiation. A simple inexpensive test was developed at BNL involving the use of static "U-bend" samples exposed to air and gamma radiation. The first trial tests were made on flat HDPE strips measuring 25 cm x 2.5 cm x 0.32 cm (10" x 1" x 0.125"). The strips were bent into a U-bend shape with the oxidized surface of the plastic on the outer surface of the bend. The bending process caused cracks to form in the oxidized surface. The free ends of the specimens were held together with stainless steel nuts and bolts. The propagation of these cracks under the conjoint action of irradiation and tensile stresses was monitored for three different gamma dose rates (1). It was found that cracking was most severe at the intermediate dose rate (9.3×10^4 rad/h) and at tensile stresses lower than the maximum value that was present at the apex of the bend.

Because of the success of this type of inexpensive test, a more comprehensive set of U-bend tests were designed in order to obtain an improved statistical basis for crack initiation and propagation under stress and irradiation conditions. To efficiently use available space in the gamma irradiation facility, the new U-bend samples were smaller, and prepared from strips of HDPE measuring 10.2 cm x 1.27 cm x 0.32 cm (4" x 0.5" x 0.125"). Holes for the nuts and bolts were drilled at a distance of 1.27 cm (0.5") from the ends of the flat strips. The U-bends were prepared with the outer surfaces in three different conditions:

- Type I - the as-received oxidized condition, which will have "natural" cracks present, as a result of bending,
- Type II - as above, but with 10 mils of the oxidized surface removed with sandpaper prior to bending. This may still allow a few very fine cracks to be present, since the sanding may not remove all of the oxygen-embrittled material, and
- Type III - the as-received "non-oxidized" surface which does not crack during the bending process.

Figure 1 shows the three types of specimens attached to individual aluminum racks. Each rack holds 8 Type I, 8 Type II, and 8 Type III specimens. The three racks shown were irradiated at different dose rates, as described in the figure caption.

Table I

Cracking in Type I HDPE U-Bend Specimens
Exposed to Gamma Irradiation in Air at 10°C

Irrad. Dose (Rad)	No. of Large Cracks	No. of Small Cracks	No. of Full Penetration Cracks	Additional Cracks Close to Full Penet.
0	90	13	0	0
7.5 x 10 ⁶ (at 1.4 x 10 ³ R/h)	97	3	2	1
6.0 x 10 ⁷ (at 8.4 x 10 ³ R/h)	95	4	2	4
1.3 x 10 ⁹ (at 4.4 x 10 ⁵ R/h)	82	4	0	1

Periodic examination of the specimens confirmed the earlier findings that intermediate dose rates and intermediate stress levels were most likely to enhance crack initiation and propagation rates. Table I shows cracking information for Type I HDPE specimens, which showed the greatest tendency for cracking. Large cracks are defined as those with a length greater than one-half of the specimen width (i.e., >0.64 cm). A small crack is one with a length less or equal to one-half of the specimen width. The numbers of cracks given in Table I are the totals for each batch of 8 replicate specimens. For the large cracks, each batch of specimens has approximately 90 - most were formed during the bending process. However, it was found from periodic visual examination that a small number of additional large cracks formed during irradiation at the low and intermediate dose rate levels.

Very few small cracks are formed during the U-bending process. However, an interesting observation in Table I is that small cracks are initiated more easily in the unirradiated specimens. A total of 13 small cracks was counted for the 8 specimens, whereas for specimens being irradiated, the numbers were only 3-4.

With respect to crack depth, the deepest cracks also occurred at the low and intermediate dose rates. A total of 4 "full-penetration" cracks was counted which resulted in complete fracture of the U-bend specimens. Most of these very deep cracks were not located at the apex of the U-bend where the initial tensile stress would be highest.

In addition to crack initiation in the Type I U-bend specimens, crack initiation was recently detected in Type II and Type III specimens irradiated at the intermediate dose rate of 8.4×10^3 rad/h (Fig. 2). At the time of detection, the accumulated dose had reached 6.0×10^7 rads. The cracks observed are very fine, and located away from the highly-stressed apex of the U-bend. Moreover, cracking was less pronounced in the Type II specimens, possibly because of the complete removal of oxidized surface material by the initial surface abrasion process. No crack initiation has yet been found in unirradiated Type II and Type III specimens, or specimens irradiated at the low and high dose rates.

Uniaxial Creep Behavior

Creep tests were carried out at 20°C (68°F) using a simple dead-load system. Strains were measured continuously using LVDTs (linearly variable differential transducers). Rates of creep, ductility-at-failure, and weight increase in the specimens caused by the absorption of the test liquids during creep were all measured. Figures 3 and 4 show failure (rupture) times and ductilities as functions of applied stress and test environment. At the highest stresses (>10.34 MPa, 1500 psi) the failure times tend to converge. This is anticipated since environmental interactions with HDPE, being time dependent, will be minimized if the stress is high enough to cause early failure. Thus, at the higher stress levels, failure is controlled by the stress and not the test environment. As the stress levels are decreased, the data in Fig. 3 shows that the highest creep strengths are for air and deionized water. There is no discernable difference in stress-rupture behavior for these two environments. Turbine oil and Igepal cause a very large loss in creep life compared to air, and scintillation fluid gives an even larger reduction. It seems, however, that a threshold stress exists, below which creep failure may not occur. For scintillation fluid this appears to be in the range 6-7 MPa (900-1000 psi).

From Fig. 4 it may be seen that at the higher stresses the ductilities also tend towards a value independent of the test environment. The value appears to lie in the 55-60 percent elongation range. This again shows that, at high stresses, failure occurs too rapidly to be affected by time-dependent environmental interactions. Therefore, creep strengths and elongations-at-failure must be similar for all environments.

At the lower stress levels (below 10.34 MPa, 1500 psi) there is a major difference in creep ductility depending on environment. The ductilities for air, water, turbine oil and Igepal are all similar at any given stress level and decrease as the stress is decreased. On the other hand, the ductilities of HDPE in scintillation fluid are larger in the low stress range. At 8 MPa (1160 psi) the elongation is about 110 percent, compared to only about 10 percent for the other four environments. An examination of the failed specimens gives the reason for this behavior. In scintillation fluid, cracks that form early in the oxidized layer, do not grow rapidly compared to those for air, water, turbine oil, and Igepal. This is probably connected with the fact that scintillation fluids contain xylene and toluene, which are known to dissolve HDPE and also are absorbed into the plastic itself. It seems that the scintillation fluid is causing blunting of cracks formed in the oxidized layer, thereby preventing concentrated deformation in these locations.

Because of this, plastic deformation is more evenly distributed throughout the gage length leading to high ductility, as observed. In the cases of air, water, turbine oil, and Igepal, the cracks initially formed in the oxidized surface are large and, often, are long enough to span the width of the specimen. These cracks are regions of concentrated plastic deformation in which fast crack growth is encouraged, leading to failure at low overall ductility.

Based on an analysis of failed specimens, the following general comments may be made (2):

- a. For a given stress level, surface cracking during creep is more prevalent in liquid environments compared to air.
- b. Cracking in air and water increases as the stress is decreased. At the lower stress levels the fracture surface is essentially perpendicular to the stress axis showing that a single crack has propagated in a "brittle" fashion causing final failure. At higher stresses, the fracture is more ductile and local necking occurs leaving behind small "tails" of material at the point of separation.
- c. Cracking in oil and Igepal is not very dependent on stress, and many cracks are present at all stress levels. Final fracture is "brittle."
- d. Scintillation fluid discourages major cracking at high stresses. Failure in this situation is preceded by severe necking; cracks around the failure point are short and blunt, indicating that propagation is difficult. At the lower stresses there is a tendency towards brittle type behavior at the time failure becomes imminent. However, prior to final separation, there is significant plastic deformation and shallow necking in the sample is present, which results in high ductility.

Effect of Surface Oxidation on Creep

As mentioned previously, high-temperature rotary molding of HDPE causes oxidation to occur on the internal surface of a container. The oxidized layer in the BNL material is approximately 50 microns (0.002 inch) in thickness and exhibits lower ductility compared to non-oxidized HDPE (3). It has been shown that removal of the oxidized layer, prior to creep testing, prevents early cracking in the specimen. When such cracking is present, it leads to intense local deformation in the cracked regions, resulting in lower overall ductility and early failure (3,4).

During this study the effect of the oxidized layer on the mechanism of creep deformation was investigated. Figures 5 and 6 show creep curves for stress levels between 7.24 to 13.79 MPa (1050 to 2000 psi) inclusive. Some HDPE specimens were in the as-received (oxidized) condition and some had

250 microns (0.01 inch) of material removed from the oxidized side of the specimens prior to testing. The latter treatment is more than sufficient to remove all oxidized material. At the lowest stress levels, 7.24 to 9.65 MPa (1050 to 1400 psi) creep is initially rapid (Stage I) but eventually slows until a linear strain deformation is established (Stage II). This is true for as-received specimens as well as for specimens which had the oxidized surfaces removed (Fig. 5). Although comparisons between the two types of specimens can be made for the 8.27 MPa (1200 psi) stress level, the creep rates are essentially identical except that the as-received material failed first after 77 hours. The non-oxidized specimen is still creeping. The creep curves in Fig. 5 also show that just prior to failure, as-received specimens show an acceleration in the creep rate (Stage III) which is associated with "necking" in the specimen and imminent failure.

At stresses of 10.34 MPa (1500 psi), and higher, major differences in behavior become evident between as-received and non-oxidized HDPE. From Figs. 5 and 6 it may be seen that the initial creep rates for non-oxidized HDPE are larger than those for as-received material at any given stress. The difference becomes larger as the applied stress is increased. Stage II creep for non-oxidized specimens tends to be shorter and a very large increase in creep rate (Stage III) occurs. Observation of non-oxidized specimens during testing showed that this large Stage III strain increment did, indeed, involve local necking in the gage length but it did not lead to immediate failure, as is the case for as-received material but to a remarkable extension of the necked region as it propagated throughout the gage length. As soon as this was completed, the rate of creep again decreased giving rise to a long "Stage IV" which is not found in as-received HDPE. The important points to note are that, at very high tensile stresses, non-oxidized material will creep faster than as-received HDPE but it will have far superior ductility and rupture life. At stresses of about 8.27 MPa (1200 psi), and probably lower, the creep rates for the two materials are likely to be very similar during Stage I and Stage II creep because of limited cracking in as-received HDPE at low strains. However, after very extended creep, when cracking starts to become important, non-oxidized material should give greatly improved creep performance.

In summary, based on data, obtained from a single batch of HDPE, removal of the oxidized layer from HDPE will likely yield the following changes in creep behavior in air when compared to as-received material:

- a. It will greatly increase the time-to-failure by about one order of magnitude for a given stress level.
- b. It will increase the creep rate during Stage I and Stage II deformation, but not in an unacceptable way.
- c. It will increase the elongation at failure by a factor of about six at the higher stresses and about four at the lower stresses.

DISCUSSION

HDPE failure under a mechanical stress is closely associated with the presence of surface cracks. For example, the U-bend specimen data, given in Table I, show that large cracks may grow under the conjoint action of tensile stresses and gamma radiation. For creep deformation, cracks also grow, with the severity of cracking and the ductility being dependent on the test environment and stress level.

From the information in the sections above, the following general mechanisms for creep failure in HDPE emerges. At low stress levels, where environmental interactions are important, two types of behavior may be expected:

- a. Environmental stress cracking behavior, where liquids such as turbine oil and Igepal cause cracks to grow quickly in a brittle manner giving rise to low ductilities. Mechanisms for environmental stress cracking involve factors such as crack front wetting effects which prevent mechanical damage at a crack front from healing. This, in turn, slows the rate of crack growth (5,6).
- b. For liquids such as scintillation fluid, containing xylene and toluene which can dissolve HDPE, any cracks forming at low stresses are blunted so that their propagation is severely retarded. Deformation is, therefore, more uniformly distributed along the specimen gage length giving high ductilities. Failure eventually occurs mainly through necking.

Air does not have surface wetting characteristics, such as water has, and cracking is less likely, as was found in this study. Nevertheless, one crack will eventually propagate and cause "brittle" behavior at the lower applied stresses.

When oxidized surface material is removed from specimens prior to creep, the ability to nucleate cracks is almost entirely prevented and elongations of up to about 600%, and higher, are possible in air at high-stress levels (Fig. 6). It should be noted, however, that even if oxidized material is removed prior to creep testing, the test environment may still control the time-to-failure and the ductility. This is clear from the few tests summarized in Table II.

Table II

Effect of test environment on the creep of non-oxidized HDPE

Specimen	Test Environment	Stress MPa (psi)	Failure Time (h)	Elongation (%)
323	Air	10.34(1500)	7704	248.9
327	DIW	10.34(1500)	452	85.2
340	Igepal	10.34(1500)	312	97.3
329	Igepal	9.65(1400)	476	59.4
330	LSF	9.65(1400)	29	76.0

The effects of radiation on plastic behavior are generally known. Usually, irradiation causes increases in strength and losses in ductility. This behavior has been confirmed for HDPE for both tensile and creep behavior (3,7). Strengthening is associated with irradiation-induced cross-linking of the polymer chains, which makes the material much more rigid and strong. Observations on embrittlement and cracking in the U-bend samples may be generally explained by ductility loss mechanisms. It would be expected that cracking of stressed U-bend specimens would increase with irradiation dose. The data in Table I, indeed, confirm this. As the irradiation dose (and dose rate) are increased, the number of large cracks increased compared to unirradiated U-bends, which showed no major cracks. A discrepancy in this model appears to exist, however, at the highest dose rate where only one large crack was found. It is possible that this could be caused by irradiation-induced chain scission which, at high dose rates, could lead to rapid stress relaxation in addition to changes in polymer chemistry. In fact, at high doses ($\sim 10^3$ rad) the HDPE samples tend to become sticky, indicating chemical instability. If stress relaxation occurs rapidly enough, crack initiation and propagation should be impeded, as was found in this work (Table I).

The large number of small cracks in non-irradiated samples (Table I) is consistent with the presence of high tensile stresses which are not decreased by irradiation-induced chain scission. Because of this, relatively large numbers of cracks are initiated, but the absence of embrittlement by irradiation prevents them from growing rapidly.

The presence of oxygen during irradiation should also be fully addressed if a detailed knowledge is to be gained on irradiation effects. It has been shown that gamma irradiation in the absence of oxygen does not cause major losses in ductility because irradiation-induced oxidation of HDPE is avoided (8).

In summary, the main failure modes for HDPE nuclear waste containers are found to be connected with specific chemical environments and gamma irradiation. These factors promote crack initiation and propagation, leading to early failure. Container life may be extended by eliminating, if possible, the damaging environments, reducing the stresses on the container, and removing the oxidized surfaces which are usually formed during container molding.

ACKNOWLEDGEMENTS

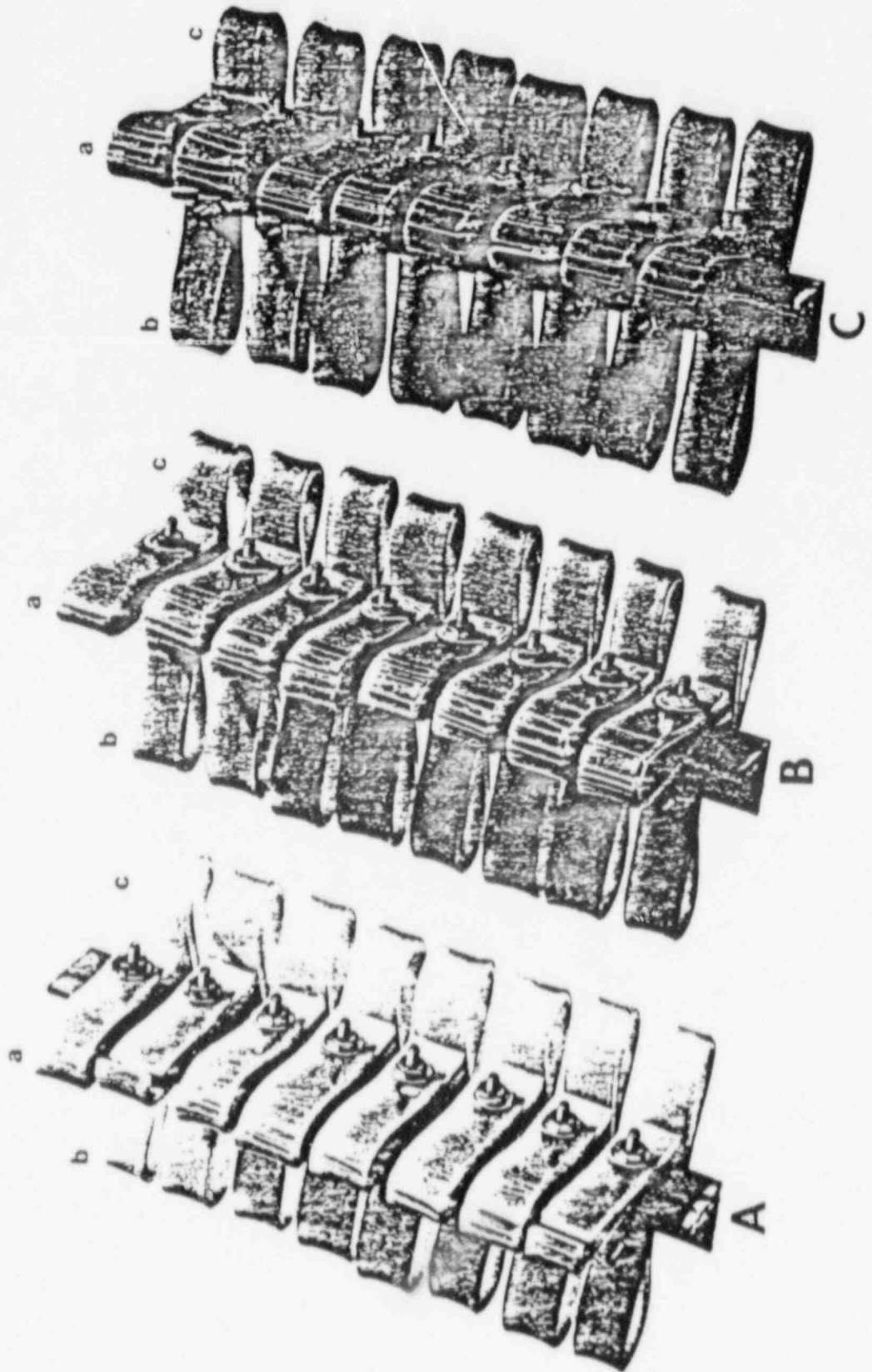
This work was performed under the auspices of the U. S. Nuclear Regulatory Commission. C. I. Anderson performed much of the laboratory work and A. Lopez was responsible for preparing the manuscript.

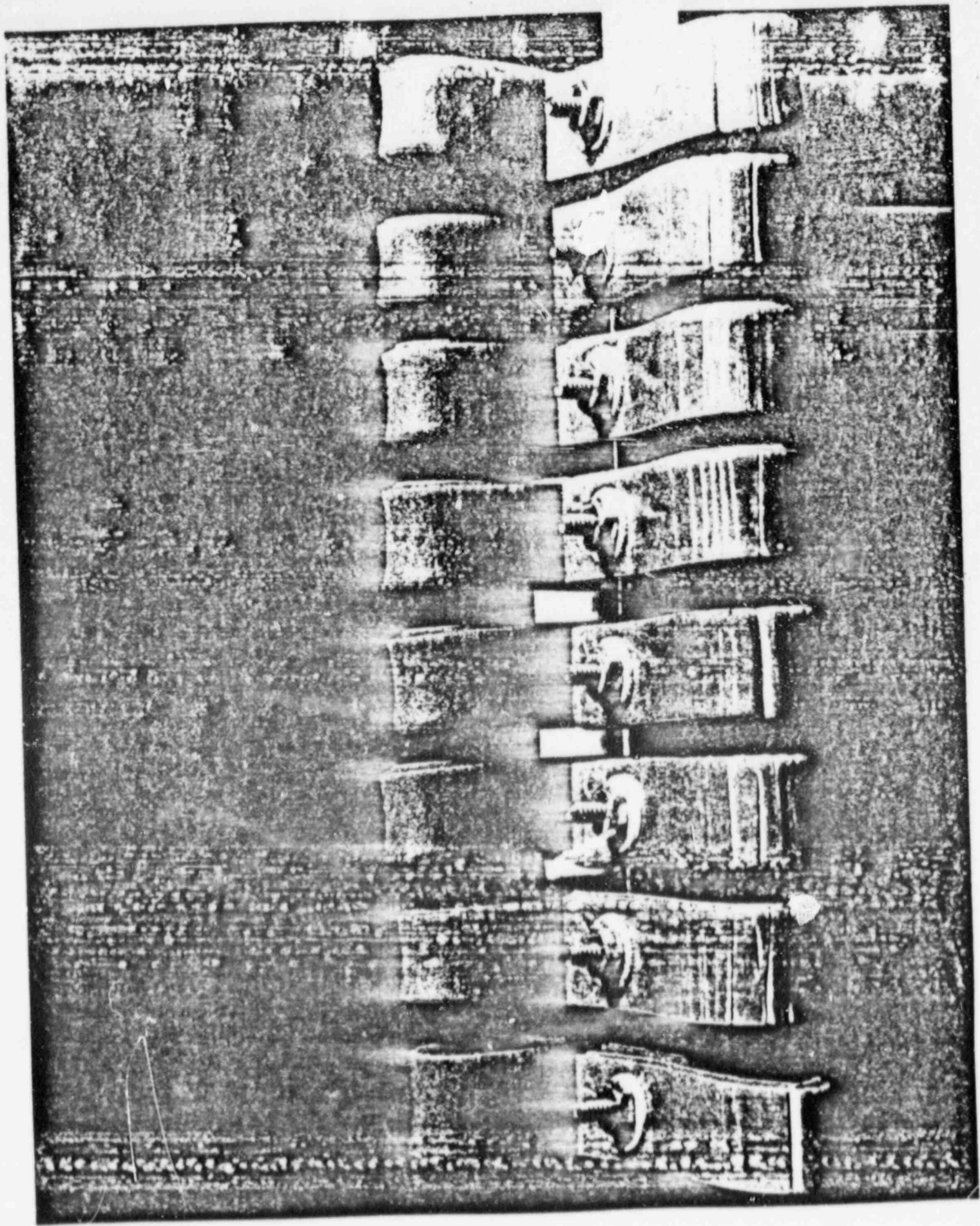
REFERENCES

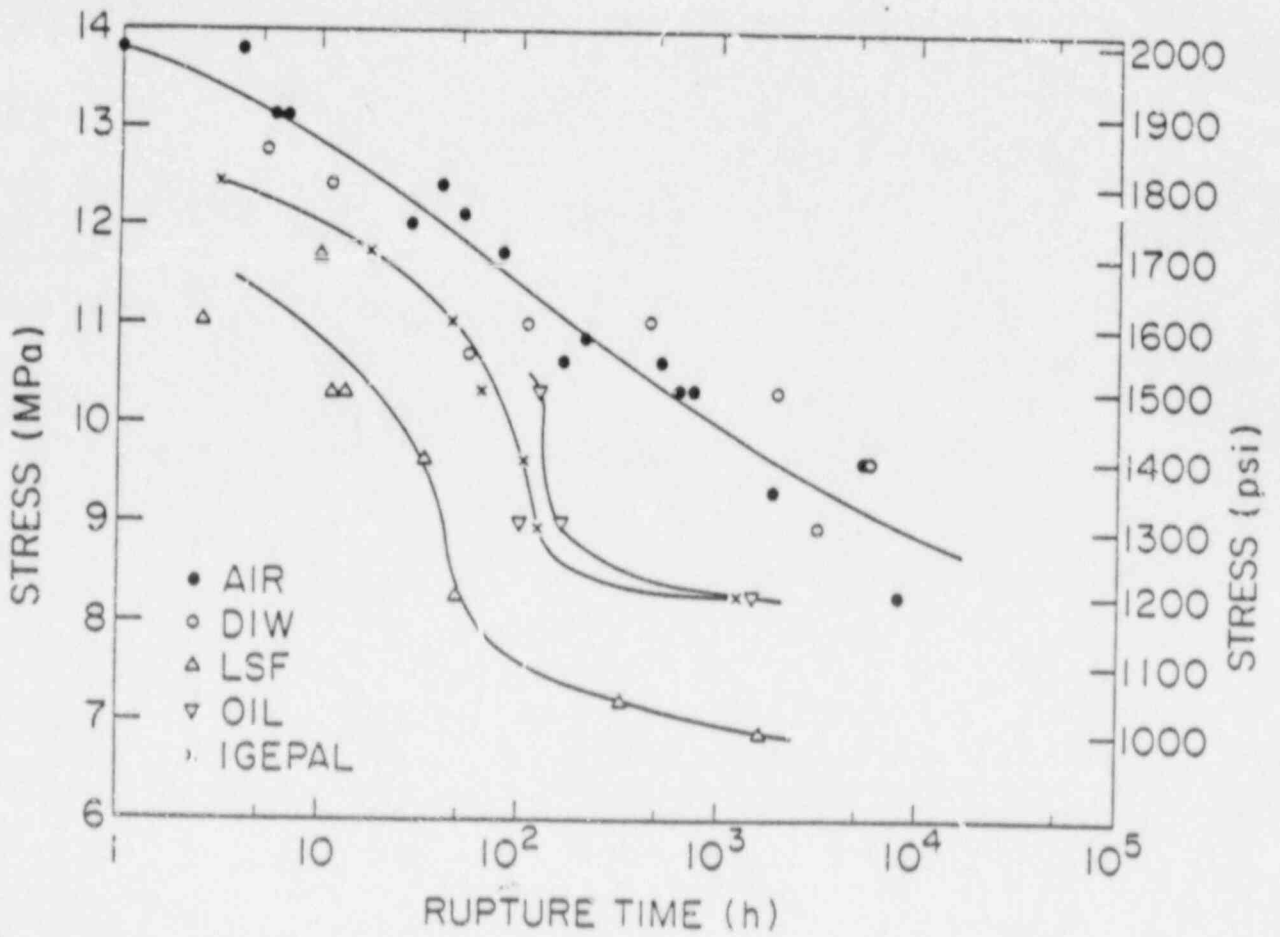
1. P. Soo and others, "Low-Level-Waste Package and Engineered Barrier Study," Quarterly Progress Report for Period January-March 1987, WM-3291-3, Brookhaven National Laboratory (1987).
2. P. Soo and others, "Low-Level-Waste Package and Engineered Barrier Study," Quarterly Progress Report for Period July-September 1987, WM-3291-5, Brookhaven National Laboratory (1987).
3. P. Soo and others, "The Effects of Environment and Gamma Irradiation on the Mechanical Properties of High Density Polyethylene," NUREG/CF 4607, Brookhaven National Laboratory (1986).
4. B. Terselius, V. W. Gedde, and J. F. Jansson, "Structure and Morphology of Thermally Oxidized High Density Polyethylene Pipe," NUREG/CR-4607, Brookhaven National Laboratory (1986).
5. M. E. R. Shanahan and J. Schultz, "Environmental Stress Cracking of Polyethylene: Criteria for Liquid Efficiency," J. Polymer Sci., 17, 705 (1979).
6. M. E. R. Shanahan and J. Schultz, "Correlation Between Environmental Stress Cracking and Liquid Sorption for Low-Swelling Liquids," J. Polymer Sci., 18, 19 (1980).
7. D. R. Dougherty and others, "An Evaluation of the Effects of Gamma Irradiation on the Mechanical Properties of High Density Polyethylene," NUREG/CR-3898, Brookhaven National Laboratory (1984).
8. R. L. Clough and others, "Accelerated-Aging Tests for Predicting Radiation Degradation of Organic Materials," Nuc. Safety, 25, 238 (1984).

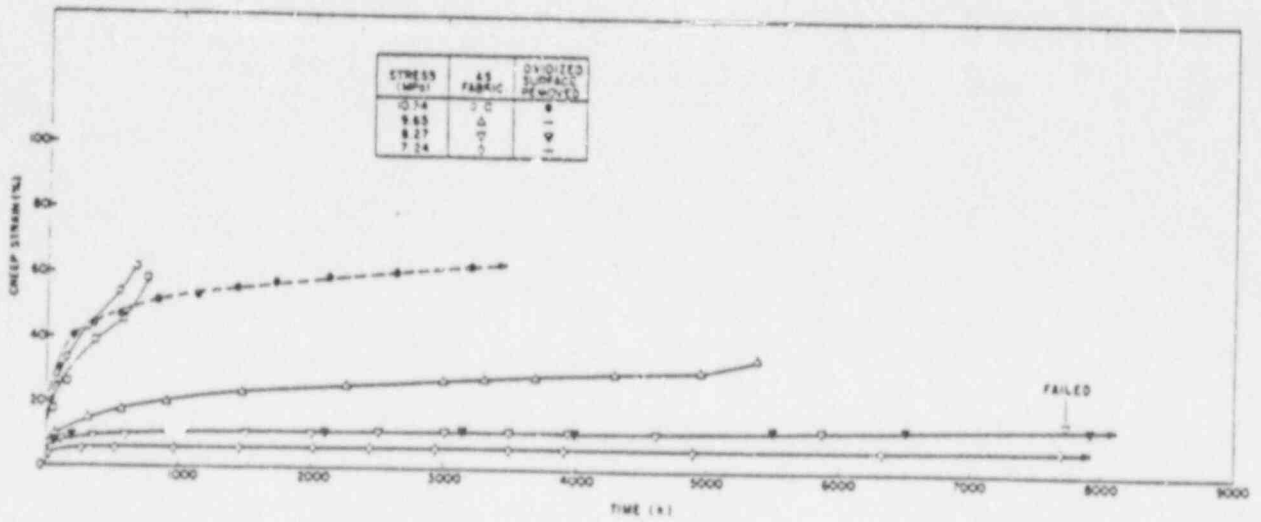
FIGURE CAPTIONS

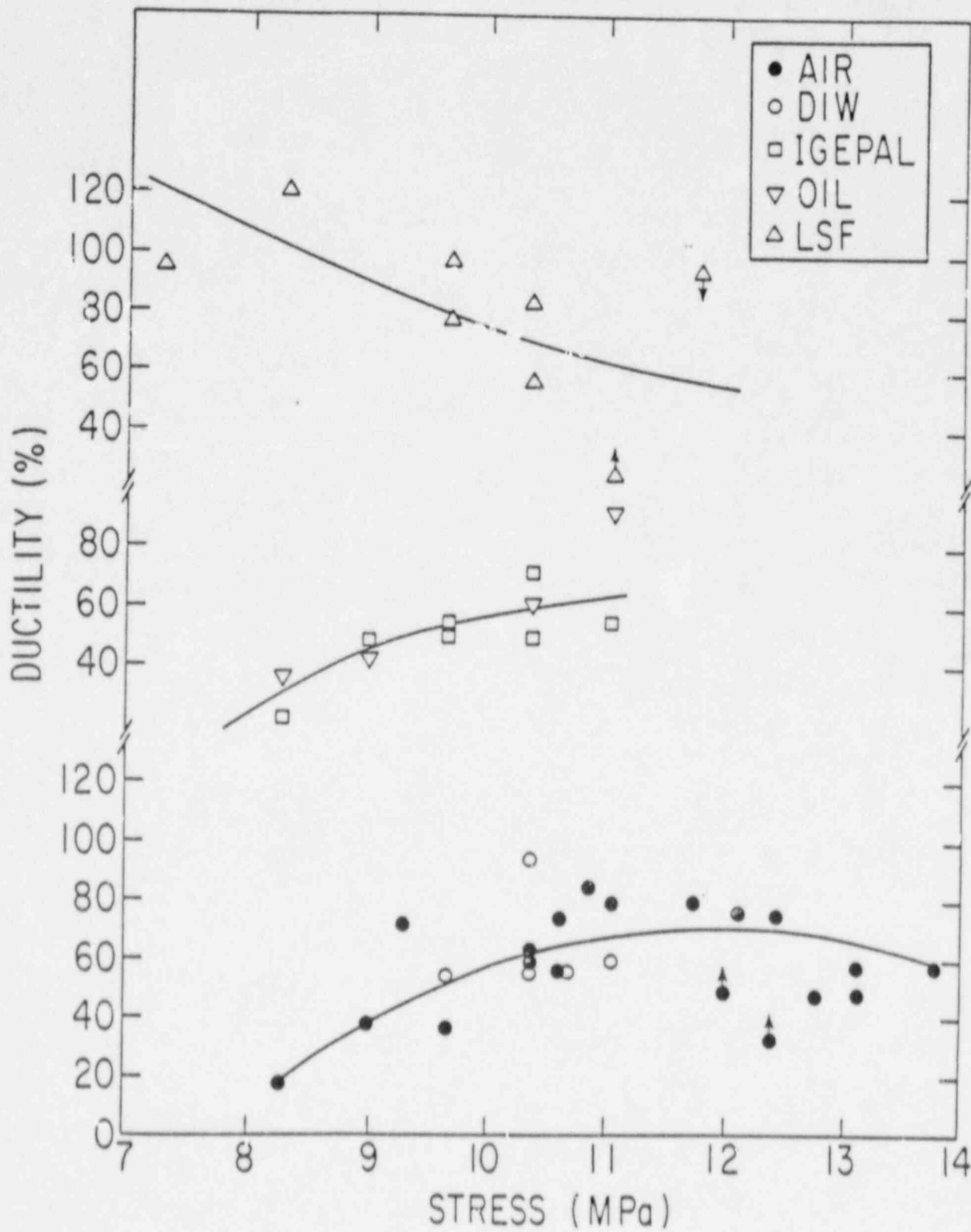
- Fig. 1 Appearance of Type I (a), Type II (b) and Type III (c) Marlex CL-100 HDPE U-Bend Specimens Gamma Irradiated to 7.5×10^6 rad (A), 6.0×10^7 rad (B), and 1.3×10^9 rad (C).
- Fig. 2 Severe cracking in Type I Marlex CL-100 HDPE U-Bend Specimens (Foreground) and Fine Cracking in Type III Specimens After Gamma Irradiation to a Dose of 6.0×10^7 rad.
- Fig. 3 Stress-rupture results for Marlex CL-100 HDPE tested in Various Environments at room temperature.
- Fig. 4 Ductility of Marlex CL-100 HDPE during creep testing in various environments.
- Fig. 5 Effect of surface oxidation on the creep of Marlex CL-100 HDPE in air at stresses between 7.24 and 10.34 MPa (1050 and 1500 psi), inclusive.
- Fig. 6 Effect of surface oxidation on the creep of Marlex CL-100 HDPE in air at stresses between 11.03 and 13.79 MPa (1100 and 2000 psi), inclusive.

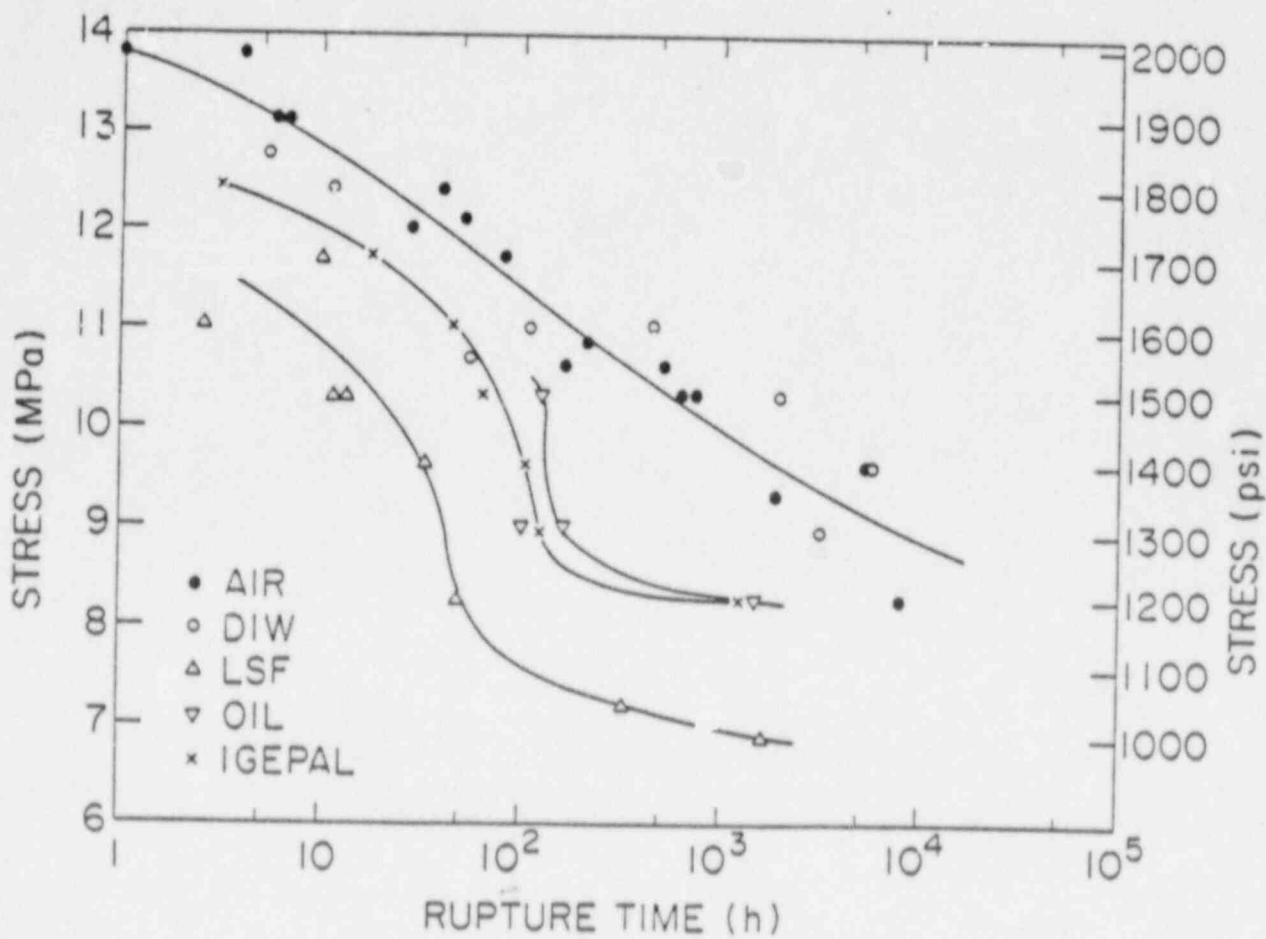


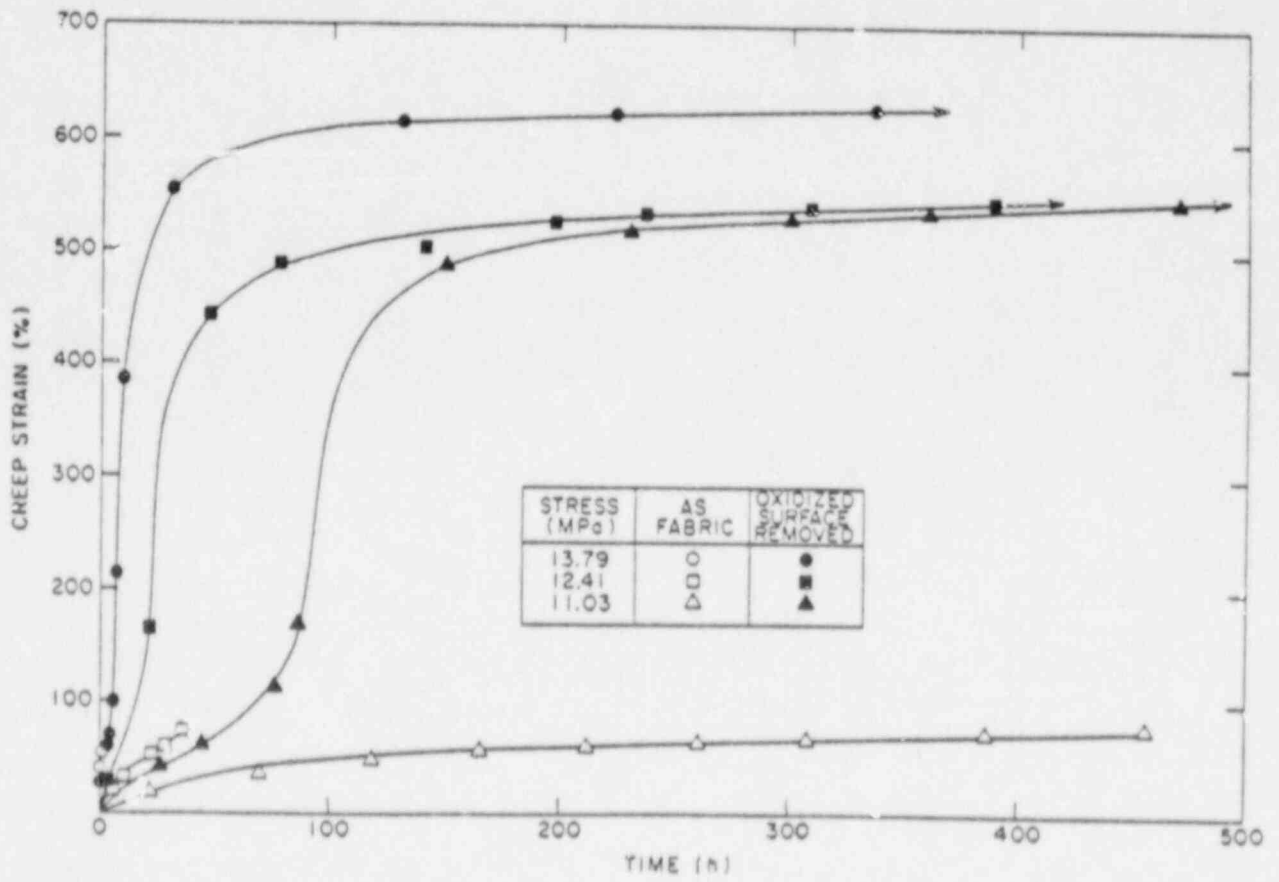


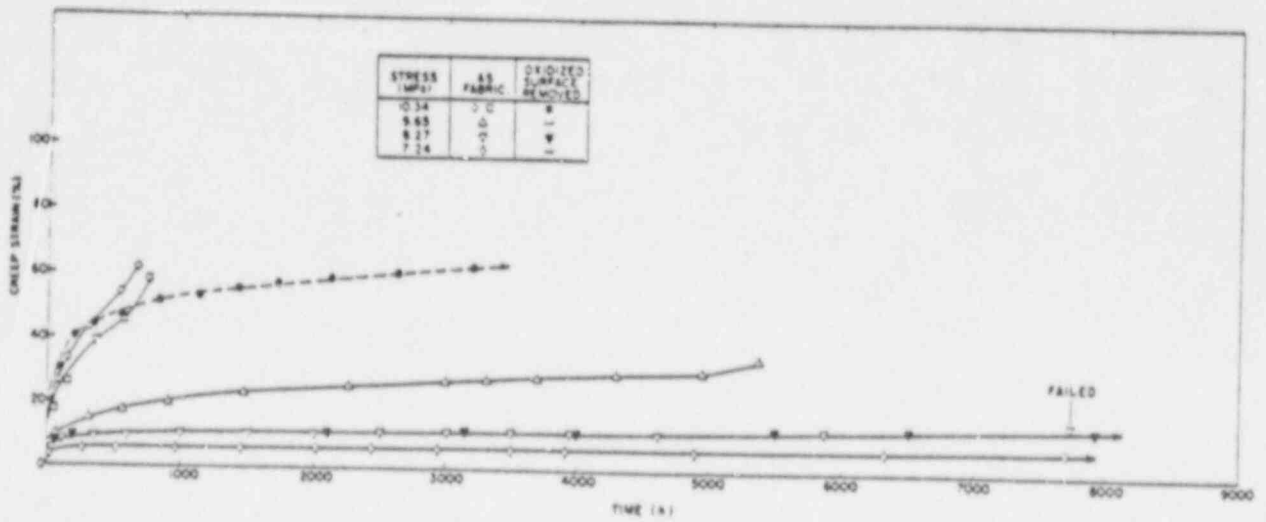












APPENDIX II

BIODEGRADATION OF ION-EXCHANGE MEDIA*

B. S. Bowerman, J. H. Clinton, S. R. Cowdery
Brookhaven National Laboratory
Upton, New York 11973

INTRODUCTION

Nuclear power plants use organic ion-exchange materials for coolant chemistry control and removal of radioactive contamination from liquid wastes (1,2). These materials may be in the form of resin beads when ion exchange only is required, or powdered resins, if filtration is needed in addition to ion exchange properties. In the latter case, other filtration media, e.g., cellulosic materials, may be mixed with the powdered resins. While a wide variety of organic polymer based ion-exchange materials are commercially available, the most widely used are polystyrene polymers with divinyl benzene cross-linking.

Waste ion-exchange resins and waste filter media containing powdered resins are disposed of after solidification with binders such as cement or after dewatering in containers. Containers for dewatered resins may be either carbon steel liners or high density polyethylene high integrity containers (HIC) (3).

Several incidents involving dewatered ion-exchange resins and dewatered filter media have occurred in recent years, both during the dewatering process and during transport to the disposal site (4). In one incident, in January 1983, ion-exchange resins underwent an exothermic reaction during dewatering. Autoxidation appeared to be the likely cause of the exotherm, but biodegradation and/or metabolic by-products of biodegradation were believed to have contributed to the initiation of the exotherm.

Another incident involving powdered ion-exchange resins in a HIC occurred in September, 1984. The HIC became pressurized during transport to the disposal site. Subsequent measurements of CO₂ generation were made using a sample obtained from the same waste batch before it was shipped. It was concluded that pressurization of the HIC could have been caused by biodegradation (4).

While a significant body of information is available on the effects of irradiation on organic ion-exchange media (5-9), there is little known regarding the effects of biodegradation on these materials. Indeed, there are limited data available on the chemical characteristics of waste ion-exchange materials (8,9). In a preliminary study conducted at Brookhaven National Laboratory (BNL) (10), Francis and Quinby examined ion-exchange resin samples collected from the BNL High Flux Beam Reactor (HFBR). CO₂ generation from the resins was measured, and two bacterial strains were isolated.

*Work conducted under the auspices of the Nuclear Regulatory Commission.

The purpose of this study was to investigate further the potential for ion-exchange media (resin beads or powdered filter media) to support biological growth. A mixed microbial culture was grown from resin wastes obtained from the BNL HFBR by mixing the resins with a nutrient salt solution containing peptone and yeast extract. Bacterial and fungal growths appeared in the solution and on the resins after 7 to 10 days' incubation at 37°C. The mixed microbial cultures were used to inoculate several resin types, both irradiated and unirradiated.

EXPERIMENTAL

The two phases of this study consisted of (a) developing a mixed microbial culture from HFBR resin wastes, and (b) determining the ability of the culture to grow on different resin types.

Two types of resin were obtained from filter units servicing the fuel storage canal of the HFBR. Both samples were obtained by scooping material from the tops of resin beds just prior to a scheduled resin replacement in January, 1987. The samples were transferred to screw-topped plastic bottles in which they were stored until needed for this study. Aseptic techniques were not used for collection of the resins. Both samples contained radioactive contamination.

Cation bead resins were obtained from a pre-filter unit and consisted of Amberlite IR-200 resins (Rohm and Haas). The resins had been in service since February, 1984. They were an amber color and contained a noticeable quantity of white particulate matter. Mixed cation/anion bead resins were obtained from the main demineralizer unit. The HFBR mixed resins were originally obtained from Graver Company and consisted of Amberlite IR-200 cation resins and Amberlite IRA-400 anion resins, or equivalents. They had been in service since June, 1985.

The mixed microbial cultures were prepared by adding samples of the HFBR resins (3-5 grams) to flasks containing 100 ml of nutrient salts medium with a secondary carbon source. The composition of the nutrient salts medium is listed in Table I. The flasks were maintained under aerobic conditions using cotton plug closures, and incubated at 37°C. Six flasks were prepared: three using the HFBR mixed resins and three using the cation resins. One flask containing each resin type was sterilized in an autoclave to provide a comparison for visual observations.

Microbial growth developed in the HFBR resin cultures after 7 to 10 days (see below for details). These cultures were then used to provide inocula for culture tubes containing the nutrient salts solution in which the normal carbon source of yeast extract and peptone had been replaced by the addition of one of several types of ion-exchange bead resins. The purpose of this second stage of testing was to evaluate the ability of the mixed cultures to utilize ion-exchange media or organic ions sorbed on the media as a carbon source.

Culture tubes containing 0.25 g of the test resins and 5 mL of the nutrient salts medium were inoculated with the mixed microbial culture grown from the HFBR resins. The nutrient medium was identical to that shown in Table I, except that the peptone and yeast extract were excluded so that the

Table I
Composition of Nutrient Salt Solution

Ingredient	Amount
$(\text{NH}_4)_2\text{SO}_4$	1.32 g
Na_2HPO_4	1.42 g
KH_2PO_4	0.54 g
$\text{MgSO}_4 \cdot 7\text{H}_2\text{O}$	0.50 g
$\text{Ca}(\text{NO}_3)_2$	0.50 mg
$\text{FeSO}_4 \cdot 7\text{H}_2\text{O}$	0.50 mg
Peptone	0.10 g
Yeast extract	0.10 g
Deionized water	to 1000 mL

only carbon available was the ion-exchange medium. Transfers were made aseptically with a microbiological transfer loop. Mixed microbial cultures from both HFBR cation and mixed resins served as inocula. Additional inoculations from the sterilized control flasks served to confirm that all transfers were aseptic and provided a basis for visual observations of growth.

Two types of mixed resin beads (LOMI and IRN) and one filter medium (EX) were evaluated. All were equilibrated with the nutrient salts medium (minus peptone and yeast extract) to expend ion-exchange sites before being placed in the test tubes. Additional tests were conducted with LOMI and IRN resins equilibrated with organic acid anions and ferrous ions to simulate decontamination wastes. Descriptions of these materials are provided in Table II.

LOMI stands for Low Oxidation State Metal Ion and represents a dilute chemical process whereby a reagent containing picolinic acid and formic acid is added to coolant water to decontaminate cooling systems in nuclear power plants. The dilute chemicals are removed from the water with ion-exchange resins. Cations are removed with a "standard" strong acid cation resin such as IRN-77 (Rohm and Haas), while picolinic and formic acid anions are collected on weak base polyacrylic anion resins, i.e., IONAC A-365 (Sybron).

The two sets of LOMI resins had been prepared for use in another BNL study (1) and consisted of mixtures of two parts IONAC A-365 to one part IRN-77. One set of resins (LL) had been "loaded" with picolinic and formic acid. For this study, the resin mixture was equilibrated with ferrous sulfate solution. The other set (LC) in "as-received" condition was equilibrated with the nutrient salts mixture.

In addition to the LOMI process, other decontamination processes are available which utilize different organic acid reagents. The more commonly used chemicals are ethylenediamine-tetraacetic acid (EDTA), citric acid, and oxalic acid, usually in combination. After decontaminations are completed, the water streams are cleaned up by ion-exchange resins.

Table II
Resin Types Evaluated for Biodegradation Potential

Designation	Description
LC	LOMI resins equilibrated with nutrient salt solution (IONAC A-365: IRN-77 = 2:1)
LL	Simulated LOMI decontamination resin wastes (picolinic acid and formic acid anions on IONAC A-365, ferrous ion on IRN-77)
IRN	IRN-77 and IRN-78 resins, equilibrated with nutrient salts (IRN-78:IRN-77=1:1)
EOC	Simulated decontamination wastes (EDTA, oxalic and citric acid anions on IRN-78; ferrous ion on IRN-77)
EC	As in EOC, but without oxalic acid
EX	Ecodex filter medium equilibrated with nutrient salt solution
N	Blank: nutrient salt solution, no carbon source

Two simulated decontamination resin wastes were prepared: one containing all three organic acids (EOC), and one with EDTA and citric acids sorbed on the resins (EC). Both simulations consisted of a one-to-one mixture of cation to anion resins (IRN-77 and IRN-78), respectively. Before mixing, the cation resins had been equilibrated with ferrous sulfate, and the anion resins were loaded with the appropriate organic acids. The organic acids were sorbed onto the resins by equilibrating a solution of equimolar amounts of the acids with the resins.

A duplicate set of all the bead resin types was prepared and subjected to gamma radiation; the total dose was approximately 100 Mrad. These samples were tested to determine whether radiation-damaged resins would provide a better carbon source for the mixed microbial culture.

RESULTS AND DISCUSSION

Both cation and mixed HFBR resins provided a ready source of microorganisms for additional tests. Addition of the resin wastes to sterile solutions containing nutrient salts and a secondary carbon source resulted in visible evidence of growth in the solutions and on the resins as summarized in Table III. Bacterial growth, indicated by turbidity in the solutions, appeared within 4 to 6 days in the flasks.

With the exception of one of the flasks containing mixed resins (AM-1), all the HFBR resins exhibited fungal growth. The fungi grew in tufts or

clumps either attached to the resins or floating in the medium. Microscopic examination of the fungal growth showed that the mycelium was composed of hypha (filaments), which had no septa (cell wall divisions). Spores from the fungal growth were similar in all the flasks containing it, suggesting that only one type of fungi was present in the HFBR resin wastes.

Preliminary characterizations of the bacterial growth in the HFBR resins has been reported elsewhere (12). At least nine distinct types of bacteria were isolated by streak plate subculture. Gram-staining and microscopic examination showed that all bacteria were rod-shaped; five were gram-negative.

Table III

Growth of Mixed Microbial Culture from HFBR Resins

Flask No. ^a	Observations and Types of Growth	Time to Develop
AC-1, AC-2	very turbid solutions; scum floating on solution surface	4-6 days
	slight fungal "halo" just above resin surfaces	8-10 days
AC-C	turbid solutions, no signs of growth	
AM-1, AM-2	turbid solution, small tufts of fungal-like growth on resins (AM-2 only)	4-6 days 20-25 days
AM-C	clear and colorless, no signs of growth	

^aKey:

A = aerobic medium and cotton stopper,

C = cation resins from HFBR

M = mixed resins from HFBR.

Numbers after hyphen are replicates. C after hyphen indicates control sterilized after preparation for visual comparisons.

The development of a mixed microbial culture is significant in that it shows that a variety of microbes (both bacteria and fungi) will be present in resin wastes. Furthermore, these micro-organisms can remain viable for some time. Several sets of cultures were obtained from the HFBR resins over a period of five months. The first culture was started after the resins had been stored at room temperature in sealed containers for one month. After the removal of samples for the cultures, the containers were resealed and opened again as needed at three, four, and five months.

Microbial growths in the test tubes containing the different resin types varied considerably. All the test tubes containing ion-exchange media and nutrient salt solution exhibited some signs of microbial growth within a week or two after inoculation. In many cases, visible growth was limited to the surface of the liquid in the test tube. In those tubes with the heaviest

growths, the solutions were turbid, and fungal mycelial masses grew directly on and above the resin surfaces. Tables IV and V list the types of growth observed in unirradiated and irradiated samples, respectively.

Fungal growth (mycelia) occurred at the liquid surface in the test tubes, including the blank tests (N) which contained nutrient salt solution and no carbon source. The reason for growth in the latter case is not obvious. It may have been due to trace amounts of organic carbon in the water used to prepare the solution or adsorbed on the test tube glass surface, or there may have been enough carbon carried on the transfer loop to support a small amount of fungal growth initially. The fungal growths at the liquid surface in tubes containing resin beads and exhibiting growth in the solution or on the surface was generally heavier than that observed in the blank tests.

Table IV
Characteristics of Microbial Growth in Test Tubes with
Unirradiated Resins

Resin Type	Inoculum Source	
	HFBR Cation Resins	HFBR Mixed Resins
LC	mycelia at liquid surface; slight turbidity in solution	mycelia at liquid surface and on resin beads; clear solution
LL	mycelia and nodules at liquid surface	mycelia at liquid surface
IRN	mycelia and nodules at liquid surface	mycelia at liquid surface
EOC	mycelia and nodules at liquid surface; turbid, green-tinted solution; mycelia and white granular material on resin surfaces	mycelia at liquid surface; turbid, green-tinted solution; mycelia and white granular material on resin surfaces
EC	same as EOC	same as EOC; definite mycelia growth on resin surfaces
EX	mycelia and nodules at liquid surface	mycelia at liquid surface
N	mycelia and nodules at liquid surface	mycelia at liquid surface

Table V

Characteristics of Microbial Growth in Test Tubes with Irradiated Resins

Resin Type	Inoculum Source	
	HFBR Cation Resins	HFBR Mixed Resins
LC	mycelia and nodules at liquid surface	no visible growth
LL	mycelia and nodules at liquid surface	no visible growth
IRN	mycelia and nodules at liquid surface; mycelia on resin surfaces	mycelia at liquid surface; mycelia on resin surfaces
EOC	mycelia and nodules at liquid surface; turbidity, floc and fungal growth in solution; mycelia and white granular material on resin surfaces	mycelia at liquid surface; turbidity, floc and fungal growth in solution; mycelia and white granular material on resin surfaces
EC	same as EOC	same as EOC

Except for the growths at the liquid surface, there were no marked growth differences between tubes with the same test resin and "different" inocula. In other words, inoculation with mixed microbial cultures from the HFBR cation resins did not result in growths that were drastically different compared to cultures from the HFBR mixed resins. However, at the liquid surface, inoculations from cation resins resulted in fungal mycelial growths and compact white nodules. Microscopic examination of the nodules showed dense aggregates of mycelia and bacteria. Tubes inoculated from the HFBR mixed resin did not have the nodules present.

Visible growth directly on or above the ion-exchange media would be more indicative of the biodegradation of the material. The heaviest fungal growth (mycelia) was observed in the solutions and on resin surfaces in test tubes containing mixed IRN resins loaded with EDTA, citric acid, and oxalic acid (EOC and EC). The solutions in these tubes were turbid, which may indicate extensive bacterial growth as well. A small amount of white granular material was present on the resin surfaces in the control samples in these tests. Clumps of mycelia in the test samples included a similar floc, or precipitate. IRN resins with no organic anions on them had similar but smaller amounts of growth develop in the same two week period.

LOMI resins exhibited small amounts of fungal growth on the resins equilibrated with nutrient salts (LC). However, the resins containing picolinate, formate, and ferrous ion (LL) showed no visible signs of growth.

Fungal growth and turbidity was more pronounced in the irradiated EOC, EC, and IRN resins, compared to the unirradiated samples. The opposite effect was seen in the LOMI resins (LC); irradiated LC samples had no fungal growth on resin surfaces.

After 2 to 3 weeks, streak plates from cultures of each resin-type were prepared on nutrient broth agar. Either bacterial or bacterial and fungal growth was obtained from all cultures, including those with no added carbon source, that had received inocula from flasks containing live microbes. Thus, although culture conditions might not be suitable for growth, bacterial and fungal cells or spores remained viable within the culture medium.

The heavy growths observed may not represent the "real world" waste situation, since excess water and the full spectrum of inorganic nutrient salts were provided. However, the fact that a mixed microbial culture was derived from real HFBR resin wastes suggests that some microbial activity is present in all dewatered resin wastes, and remains viable for at least several months.

CONCLUSIONS

The main conclusions of this study are: a mixed microbial culture can be grown from actual ion-exchange resin wastes provided nutrient salts, a secondary source of carbon, and excess water are added to the wastes, and the use of a mixed microbial culture is appropriate for evaluating the potential for ion-exchange media to support biological activity.

The effects of environmental factors such as resin type, chemicals sorbed on the resins and radiation damage were examined in this study. Heavier growths were seen in IRN resins subjected to 100 Mrad of gamma irradiation. Some organic chemicals used in dilute chemical decontamination processes encourage heavier microbial growths.

The growth evaluations in this study were qualitative. Further research quantifying the ability of micro-organisms to metabolize ion-exchange media would be useful, since biodegradation could have potentially adverse effects on the long-term stability of the wastes or waste containers. Specific topics which should be investigated include: 1) establishing the long-term viability of mixed microbial cultures in dewatered resin wastes, and 2) identifying the characteristics of respiration and metabolism of microbes in dewatered resins. The latter topic is important because the effects of biodegradation cannot be predicted accurately without basic information on how rapidly microbes utilize the nutrients available in the wastes. Specific data on microbial metabolism under expected disposal conditions, e.g., sealed containers at low (15° to 20°C) temperatures, should be obtained.

REFERENCES

1. W. E. Clark, "The Use of Ion-Exchange to Treat Radioactive Liquids in Light-Water-Cooled Nuclear Reactor Power Plants," NUREG/CR-0143, ORNL/NUREG/TM-204, 1978.
2. K. H. Lin, "Use of Ion-Exchange for the Treatment of Liquids in Nuclear Power Plants," ORNL-4792, 1973.
3. R. L. Jolley, et al., "Low-Level Waste from Commercial Nuclear Reactors, Vol. 2, Treatment, Storage, Disposal, and Transportation Technologies and Constraints," ORNL/TM-9846/V2, 1986.
4. B. S. Bowerman and P. L. Piciulo, "Technical Consideration Affecting Preparation of Ion-Exchange Resins for Disposal," NUREG/CR-4601, 1986.
5. T. E. Gangwer, M. Goldstein, and K. K. S. Pillay, "Radiation Effects on Ion-Exchange Materials," BNL-50781, 1977.
6. K. J. Swyler, C. J. Dodge and R. Dayal, "Irradiation Effects on the Storage and Disposal of Radwaste Containing Organic Ion-Exchange Media," NUREG/CR-3383, 1983.
7. K. J. Swyler, C. J. Dodge, and R. Dayal, "Assessment of Irradiation Effects in Radwaste Containing Organic Ion-Exchange Media," NUREG/CR-3812, 1984.
8. D. R. MacKenzie, M. Lin, and R. E. Barletta, "Permissible Radionuclide Loadings for Organic Ion-Exchange Resins from Nuclear Power Plants," NUREG/CR-2830, 1983.
9. P. L. Piciulo, "Technical Considerations for High Integrity Containers for the Disposal of Radioactive Ion-Exchange Resin Waste," NUREG/CR-3168, 1983.
10. A. J. Francis and H. Quinby, "Microbial Degradation of Spent Reactor Resins - A Preliminary Study," BNL-30897, 1981.
11. J. W. Adams and P. Soo, "Decontamination Impacts on Solidification and Waste Disposal," Quarterly Progress Report, October-December 1986, WM-3246-1, May 1987.
12. P. Soo, et. al., "Low-Level Waste Package and Engineered Barrier Study," Quarterly Progress Report, July-September 1987, WM-3291-5, December 1987.

3
6
HIGH DENSITY POLYETHYLENE (HDPE)

HIGH INTEGRITY CONTAINER (HIC)

REGULATORY ISSUES

Michael Tokar
Low-Level Technical Branch
June / 1988

6/18

CURRENT SITUATION

- * STATE OF SC HAS BEEN ACCEPTING HDPE HICS FOR SEVERAL YEARS AT THE BARNWELL LLW DISPOSAL FACILITY (See list of certificates of compliance).
- * NRC IS REVIEWING 3 TOPICAL REPORTS (from CNSI, TFC-Nuclear, & W-Hittman) ON HDPE HIC DESIGNS.
- * NRC CONSULTANTS AT BNL AND BROWN UNIVERSITY HAVE RAISED QUESTIONS CONCERNING ABILITY OF HDPE HICS TO PROVIDE LONG-TERM (300 yr.) STRUCTURAL STABILITY AS REQUIRED BY 10 CFR PART 61.

Certificates of Compliance

State of South Carolina

HIC Certificates of Compliance

<u>Issued to :</u>	<u>Issued what:</u>	<u>Issued when:</u>
Adwin Equipment Company	55-gallon HIC	5/29/84
Chem-Nuclear	HDPE HICs (x 14)	5/28/81
Chem-Nuclear	FRP V.C	2/23/82
Chem-Nuclear	Overpack HICs (x3)	4/8/83
Philadelphia Electric Comp.	PECO-HIC-1	9/28/81
Hittman	Radlok-55 HIC	6/17/82
Hittman	Radlok-100 HIC	6/17/82
Hittman	Radlok-200 HIC	5/5/83
Hittman	Radlok-500 HIC	9/31/85
LN Technologies	Barrier-55 HIC	9/1/83
TFC	NUHIC-120 HIC	11/1/83
NUPAC	HDPE 142 HIC	8/20/84
NUPAC	FL-50 HIC	9/26/85
Chichibu	Concrete HICs (x2)	8/12/86
Vermont Yankee	HDPE HIC	10/10/83

U.S. Energy

CHRONOLOGY OF EVENTS REGARDING NRC/NMSS INVOLVEMENT IN REVIEW OF HDPE HICS

DATE	EVENT
6/84	4 Topical reports on HDPE HIC design received.
5/85	NUS withdraws HDPE report.
6/85	NMSS Initiates T.A. at BNL for HDPE technical review.
1/86	NMSS authorizes BNL TO identify a methodology to determine structural stability of HDPE HICS.
3/86	NMSS Initiates work at BNL to develop methodology.
7/86	NUS submits report stating that HDPE HICS will not meet acceptance criteria.
4/87	BNL submits report on HDPE methodology & criteria.
8/87	NMSS notifies SLTP & States.
SUMMER/87	NMSS meets NMSS meets with vendors to discuss concerns over HDPE.
10/87	NMSS requests further info from vendors.
2/88	Vendors submit responses to request for info.
5/88	Issuing Preliminary Report on review of HDPE HICS and vendor responses.

BNL ACTIVITIES ON HDPE HICS

ANALYTICAL: (FIN A3171) DEVELOPMENT OF DRAFT METHODOLOGY (HICSEP) REPORT.

- * RECOMMENDED ACCEPTANCE CRITERIA: (1) NO BUCKLING; (2) NO TERTIARY CREEP; (3) DO NOT EXCEED ALLOWABLE MEMBRANE STRESSES.

- * USED TO MAKE SAMPLE CALCULATIONS THAT RESULTED IN PREDICTION THAT HDPE HICS WOULD EXCEED ALLOWABLE BUCKLING, CREEP, AND MEMBRANE STRESSES.

- * VENDORS ALL AGREED THE CRITERIA WERE REASONABLE.

EXPERIMENTAL: (FIN 3291): STUDY OF CRACK INITIATION AND PROPAGATION IN A GAMMA-RADIATION ENVIRONMENT, AND CREEP IN SELECTED ENVIRONMENTS.

SILLING FINDINGS

- * DESIGN AGAINST CREEP BUCKLING IS A HOPELESS TASK.
- * BECAUSE OF UNCERTAINTIES (REGARDING THE LONG-TERM DUCTILE-TO-BRITTLE TRANSITION OF HDPE), IT IS QUESTIONABLE THAT A DEPENDABLE PROJECTION (for failure stress) CAN EVER BE FOUND.
- * CREEP PROPERTIES OF MARLEX CL-100 UNDER LONG-TERM LOADING CONDITIONS ARE VIRTUALLY UNKNOWN.

SILLING'S KEY CONCLUSION

THE REQUIRED KNOWLEDGE FOR DESIGNING A HIC WITH HDPE AS THE LOAD-BEARING MATERIAL FOR A 300-YEAR LIFE GOES BEYOND WHAT STRUCTURAL MECHANICS AND POLYMER SCIENCE CAN RELIABLY PROVIDE.

POTENTIAL IMPACTS OF DISAPPROVAL OF HDPE HICS

DISPOSAL SITE IMPACTS:

- NO EVIDENCE OF IMMEDIATE THREAT TO PUBLIC HEALTH & SAFETY (Part 61 dose limits not violated).
- POTENTIAL (hard to quantify) FUTURE EFFECTS ON B, C TRENCHES NEED ANALYSIS:
 - (a) SITE IS MONITORED (wells & sumps):
SHOULD ASSESS NEED FOR INCREASED MONITORING
 - (b) NEED FOR REMEDIAL ACTION ALTERNATIVES SHOULD BE EVALUATED FOR B, C TRENCHES.

GENERATOR IMPACTS:

- SOME PLANTS CURRENTLY RELYING ON HDPE HICS.
- ALTERNATIVES (other HICS, solidification media) EXIST, BUT MAY REQUIRE TIME (months) TO SET UP.

HIGH DENSITY POLYETHYLENE HIC USAGE 1987 - 1988

1987

CLASS A - UNSTABLE	(?)
CLASS A - STABLE	409
CLASS B	255
CLASS C	40

1988

CLASS A - UNSTABLE	2
CLASS A - STABLE	245
CLASS B	138
CLASS C	33